

UltraBoard: Always-Available Wearable Ultrasonic Mid-air Haptic Interface for Responsive and Robust VR Inputs

CHANGHYEON PARK, Graduate School of Culture Technology, KAIST, Republic of Korea

YUBIN LEE, School of Computing, KAIST, Republic of Korea

SANG HO YOON, Graduate School of Culture Technology, KAIST, Republic of Korea

Free-hand interaction in VR is intuitive and easy to learn, making it applicable to fundamental interactions such as VR typing. However, the absence of haptic feedback reduces spatial awareness and immersion while performing the input, impacting accuracy and increasing fatigue. While previous works embedded haptic feedback, they either require constant contact with the skin or a desktop installation with a fixed distance. We propose UltraBoard, a novel wearable haptic interface providing ultrasonic mid-air haptic feedback for all hand regions, including fingertips. We adaptively control the phased array's position in accordance with the hand movement and location to support consistent haptic feedback for real-time VR typing input. With simulation and experiment, we designed and validated the customized ultrasound phased array to support hand input. We propose guidelines for the development of a finger-level wearable ultrasonic mid-air haptics interface and system through this process. A follow-up user study showed significant improvements in typing confidence and usability with UltraBoard. Notably, the mid-air tactile typo alert enabled with our interface enhances user experience during VR typing. Our results showed a promising approach to utilizing a mid-air haptic interface to promote confidence in VR typing.

CCS Concepts: • **Human-centered computing** → **Interaction techniques**; **Virtual reality**; • **Hardware** → **Tactile and hand-based interfaces**.

Additional Key Words and Phrases: Mid-air haptic wearables, mid-air hand interactions, always-available tactile interface, VR typing

ACM Reference Format:

Changhyeon Park, Yubin Lee, and Sang Ho Yoon. 2025. UltraBoard: Always-Available Wearable Ultrasonic Mid-air Haptic Interface for Responsive and Robust VR Inputs. *Proc. ACM Interact. Mob. Wearable Ubiquitous Technol.* 9, 2, Article 44 (June 2025), 31 pages. <https://doi.org/10.1145/3731413>

1 INTRODUCTION

Free-hand interaction in VR environments is an intuitive and user-friendly interaction method. With advancements in the performance of embedded hand tracking systems with commercialized HMDs like Meta Quest 3S [57], free-hand interaction and gesture recognition have become the main approaches to perform VR inputs [92] such as VR typing. Still, due to the potential tracking loss during hand occlusions, the user's hand must remain unobstructed within the camera's view. This limits the available workspace volume and restricts natural hand movement during interactions in VR. Moreover, the lack of haptic feedback contributes to user fatigue and diminishes the usability of the interaction [51, 66].

In particular, the absence of haptic feedback during mid-air interactions leads to reduced presence and spatial awareness. This causes high user fatigue and ultimately results in decreased usability [16, 32, 40]. Integrating

Authors' addresses: [Changhyeon Park](mailto:sac7160@kaist.ac.kr), sac7160@kaist.ac.kr, Graduate School of Culture Technology, KAIST, Daejeon, Republic of Korea; [Yubin Lee](mailto:dkch3236@kaist.ac.kr), dkch3236@kaist.ac.kr, School of Computing, KAIST, Daejeon, Republic of Korea; [Sang Ho Yoon](mailto:sangho@kaist.ac.kr), sangho@kaist.ac.kr, Graduate School of Culture Technology, KAIST, Daejeon, Republic of Korea.



This work is licensed under a [Creative Commons Attribution 4.0 International License](https://creativecommons.org/licenses/by/4.0/).

© 2025 Copyright held by the owner/author(s).

ACM 2474-9567/2025/6-ART44

<https://doi.org/10.1145/3731413>

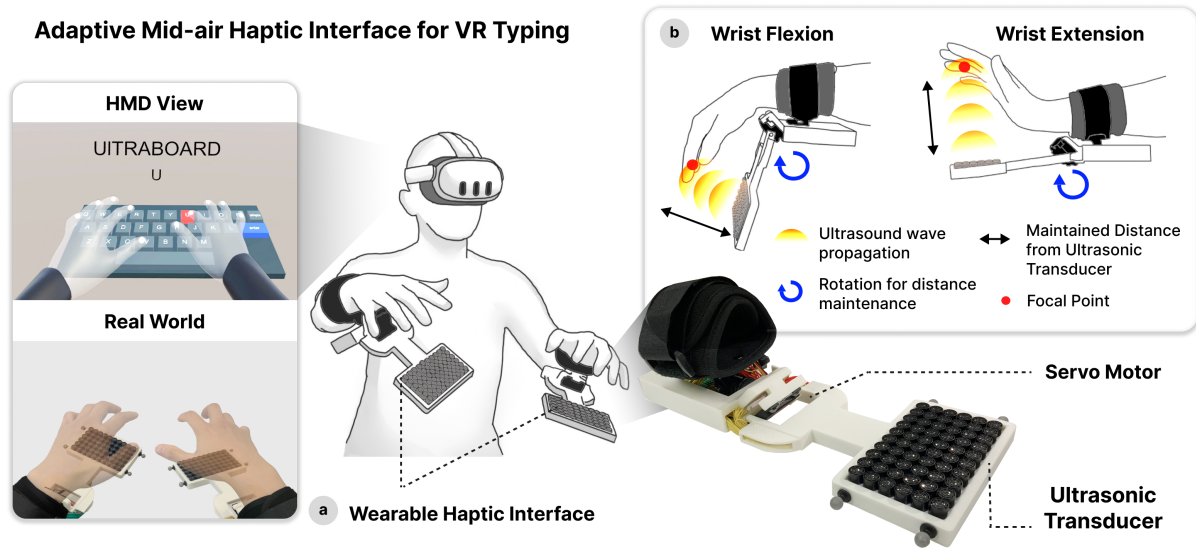


Fig. 1. Overview of Ultraboard. (a) We designed a wrist-worn mid-air haptic interface that provides tactile sensation across the entire hand. (b) Ultraboard adjusts the position of the phased array based on the spatial relationship between the hand and the array to provide consistent feedback during any hand movements and motions.

visual and tactile stimuli can significantly enhance users' perceptual levels, and providing tactile sensation during mid-air interaction has the potential to improve both user experience and usability [63, 74]. Indeed, users tend to prefer tactile feedback on their fingers while performing input, and previous work has shown enhanced immersion and realism [25].

Accordingly, researchers have suggested various haptic devices to offer a realistic sensation while minimizing user discomfort. Methods of providing tactile sensation can be categorized into contact-based and non-contact-based haptics. The contact-based approaches have the advantage of providing strong haptic feedback with precise localization [80, 83, 89]. However, these methods either require specific hand postures or limit the range of motion while in use. Moreover, contact-based approaches need to consider hardware fit for a variety of populations to maintain comfort and perceivable feedback [93].

In contrast, non-contact mid-air haptics entitle users to more freedom in range of motion with no attached hardware. Gupta et al. [27] developed AirWave that supports non-contact haptic feedback using air vortex rings. While AirWave delivered haptic feedback to specific locations, it suffered from inaccuracy and delay. Another form of non-contact haptics is the use of ultrasonic mid-air haptics (UMH) [70]. UMH creates precise focal points with approximately 8.6 mm resolution at a frequency of 40 kHz at 20°C [30] controlled with unnoticeable delay because it utilizes acoustic waves. Also, UMH supports rendering various shapes and textures. Although UMH's intensity is insufficient for delivering constant pressure, it is adequate to support tactile sensations like vibration or texture. This shows the potential of UMH as a versatile tool for interactions [34].

UMH, however, has limitations in rendering haptic feedback in terms of effective volume size due to the mechanical characteristics of ultrasonic transducers such as their directivity and size and the acoustic properties of ultrasonic waves [70]. Specifically, providing tactile effects focused on particular points requires maintaining a certain distance range between the user and the transducer array [75]. Previous studies have proposed enlarging the workspace of ultrasound transducer arrays by increasing array size [29, 59, 84], using robot arms to reposition

the array [5, 90], or employing fixed servo motors to adjust array orientation [35]. Nonetheless, these approaches still require ultrasonic transducer arrays to be installed at fixed locations, which either limits workspace flexibility or demands excessively large equipment. For the broad applicability and usability of UMH, it is necessary to develop a new interface that does not restrict user movements or positioning. A wearable form factor enables the delivery of tactile sensations without spatial constraints. However, ensuring robust UMH performance requires more than simply converting a stationary UMH interface into a wearable form. Since the new interface must be worn by the user, it is essential to minimize its size to enhance usability. Additionally, it is required to provide perceptible feedback across the entire hand, including the fingers for applicability.

In this study, we propose a novel wearable haptic interface that physically adjusts the relative position of an ultrasonic transducer array in accordance with the user's finger position to deliver uniform tactile intensity regardless of hand movement. To achieve this, we first simulated the acoustic radiation pressure to determine the appropriate shape and size of the ultrasonic transducer array for the wearable UMH. Then, we identified the effective distance range and developed an algorithm and system to maintain it. Unlike previous UMH research focusing on perception on the palm [19, 85, 94], we carried out experiments to determine the minimum perceivable UMH intensity on the fingertips. Based on the results, we designed an interface that is compact yet capable of delivering feedback with sufficient intensity to be perceived by the user. We evaluated the performance of our haptic interface for VR typing, which represents one of the most fundamental input methods with a mid-air approach. Our work shows the potential to enhance user experience and expand the application compared to conventional fixed ultrasonic transducer array-based systems. In other words, we provide essential guidelines and serve as a foundation for advancing stationary UMH systems into a wearable form. The main contributions of our research are as follows:

- We explored the size and shape of phased arrays and distance range, enabling effective finger-level wearable UMH by simulating the spatial distribution of acoustic radiation pressure.
- We proposed criteria for developing a wearable UMH form factor capable of providing feedback across the entire hand by conducting a perception study targeting the fingers.
- We validated the effectiveness of the proposed interface and system guidelines by developing and evaluating a system that provides haptic feedback during VR typing.

2 RELATED WORK

2.1 Haptic Feedback for VR Hand Interactions

In VR environments, interaction methods that rely solely on visual feedback face several limitations. The absence of tactile or kinesthetic feedback diminishes both realism and immersion [22]. Additionally, this increases cognitive load, leading to elevated levels of fatigue [67]. Moreover, in tasks that require fine motor control, the lack of haptic feedback reduces accuracy. As a result, efforts have been made to develop multimodal interaction techniques that integrate various sensory feedback, such as auditory and tactile feedback, to enhance interactivity [21, 69, 86].

For VR interactions, the integration of tactile and visual feedback improves users' perception and motor accuracy and is highly favored by participants [1, 39] compared to other multisensory feedback. Aligned with these findings, researchers have focused on building standard interaction methods by combining visual and tactile feedback. However, spatial limitations in haptic feedback delivery methods and the incompleteness of feedback still persist [76]. We propose a haptic interface capable of providing haptic feedback without spatial constraints and suitable for providing feedback to the fingers, based on measurements and simulations of the spatial distribution of haptic feedback.

2.2 Mid-air Haptics

Haptic interfaces are classified into five categories based on their mechanisms: Physical props, handhelds, wearables, encountered type, and mid-air type [93]. Physical props [8, 81] allow for intuitive and realistic haptic feedback by utilizing actual physical objects, enabling users to understand how to use them naturally without additional training. Moreover, they are relatively simpler and more cost-effective to implement compared to complex electronic or mechanical haptic systems. However, they are designed for specific scenarios, making it challenging to generalize them for diverse scenarios and interactions. Additionally, they are limited compared to electronic or mechanical haptic technologies when it comes to dynamic or complex feedback, potentially reducing immersion. Furthermore, physical props are challenging to personalize to suit different users' physical characteristics or preferences. Handheld devices [3, 7, 9, 10, 31, 47], commonly implemented along with commercial controllers, offer a wide range of haptic feedback while keeping a small form factor. However, the requirement for users to constantly hold a handheld device presents a significant limitation. This restricts hand freedom and necessitates maintaining specific postures, reducing the flexibility of use and experience, which can ultimately diminish the sense of immersion. On the other hand, wearable devices [18, 67, 68, 73, 96] allow natural movement of the user while providing diverse haptic feedback. However, wearing equipment that directly contacts the user's body, like VR suits or gloves, for long periods tends to incur discomfort due to sweat and fatigue, potentially impacting overall user experience and usability. Additionally, differences in users' body types and sensitivity levels make it challenging for standardized designs to suit all users effectively. Unlike wearables and handhelds, encounter-type haptic interfaces [37, 44] provide more natural feedback without requiring the user to hold or wear a device, offering a greater degree of freedom. However, they face issues related to power consumption, size, noise, and synchronization with virtual objects.

To enhance freedom of users' hand movement and eliminate the needs for equipping the devices from contact-based haptic techniques, contactless mid-air haptic approaches have been explored. Among them, UMH offers precise spatial and temporal control of haptic feedback [20] and requires a relatively simple mechanical system [36, 70]. By adjusting ultrasound modulation parameters, UMH supports various types of haptic feedback, enhancing the user's perception [49, 79]. However, UMH has limitations in the physical size of the rendered haptic feedback and the workspace, due to factors such as the power and directivity of the transducer, as well as the propagation of ultrasonic waves [70]. In other words, to provide appropriate tactile effects, a consistent distance range between the user and the transducer array must be maintained [75].

To address the workspace limitation of UMH, previous work increased the number of transducers in the array and connected array units to enhance the intensity of overlapping ultrasound waves and further expand the reachable area [29, 59, 84]. However, this solution introduces computational challenges, occupies significant physical space, and still confines the user's workspace to a fixed location. Other works involve actively manipulating the location of the array to an effective position, either using robot arms [5, 90] or a servo motor-based rotating platform [35] to expand the working interaction volume. While these methods offer a solution for enlarging the workspace of the ultrasound transducer array, they still present limitations, such as confining the array to specific positions or requiring bulky equipment setup.

In our work, we address existing challenges by proposing an adaptive wearable haptic system that controls the position of the ultrasound transducer array in real-time, providing users with perceptible tactile feedback on the hand without constraining their movement or workspace. Unlike physical props, which are limited to specific scenarios, Ultraboard offers a wider range of interactions by providing active feedback. Adjusting UMH parameters can generate various sensations and textures, including dynamic effects such as moving strokes. This enables interactions beyond simple scenario-specific feedback, such as scrolling, alerts, and directional guidance. Unlike handheld devices and wearable devices, such as a method of attaching simple actuators to lightweight data gloves [4, 77, 91], Ultraboard enables bare hand interaction by eliminating the need for direct

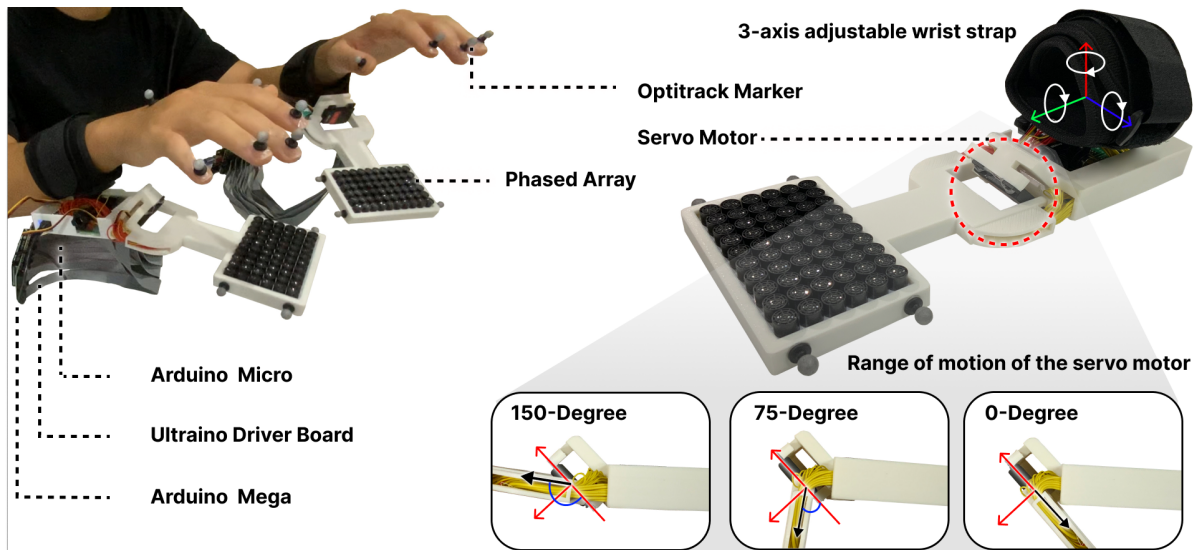


Fig. 2. Haptic interface prototype and range of motion of a servo motor. 3-axes indicate rotational adjustability to fit the wearable interface to individual users.

contact with the hand. Since direct contact between the feedback area and UltraBoard is not required, there is no need for different device sizes to accommodate variations in user body shape unlike wearable devices. This capability allows it to accommodate user variability effectively. Lastly, UltraBoard optimizes power consumption and size, differentiating it from encountered-type haptic interfaces by utilizing a minimized transducer array. And it activates only when in use, enhancing the user's freedom of movement.

2.3 Ultrasonic Mid-air Haptics in HCI

The advantages of UMH, such as its spatial and temporal precision, mechanical simplicity, and capability to deliver diverse tactile feedback through modulation parameters, have sparked extensive exploration into UMH applications within HCI. Studies have applied UMH to diverse body areas, including the face [23, 46, 58], palm [45, 79], fingers [71], and mouth and oral cavity [78], exploring how individuals perceive haptic feedback on each region. However, for the hand, most research on UMH perception has focused on the palm due to its high sensitivity [82] and larger surface area [43, 45, 79]. Research on the perception of UMH on the fingertips has been limited, despite the varying vibration detecting sensitivities to tactile sensations across different fingertips [42], and remains insufficiently explored.

By conducting a perception study on two fingertips, one highly sensitive (middle fingertip) and one less sensitive (pinky fingertip), we identify how basic UMH parameters affect the perception of haptic feedback on the fingertips. Additionally, we present a guideline for effective haptic rendering in mid-air typing contexts by conducting a user study focused on VR typing scenarios.

3 ULTRABOARD SYSTEM

We aimed to advance the existing stationary UMH into a wearable UMH supporting finger-level haptic feedback. To this end, we provide haptic feedback across the entire hand without restricting the user's workspace. However, transitioning from stationary UMH to a wearable form factor introduces challenges that must be addressed.

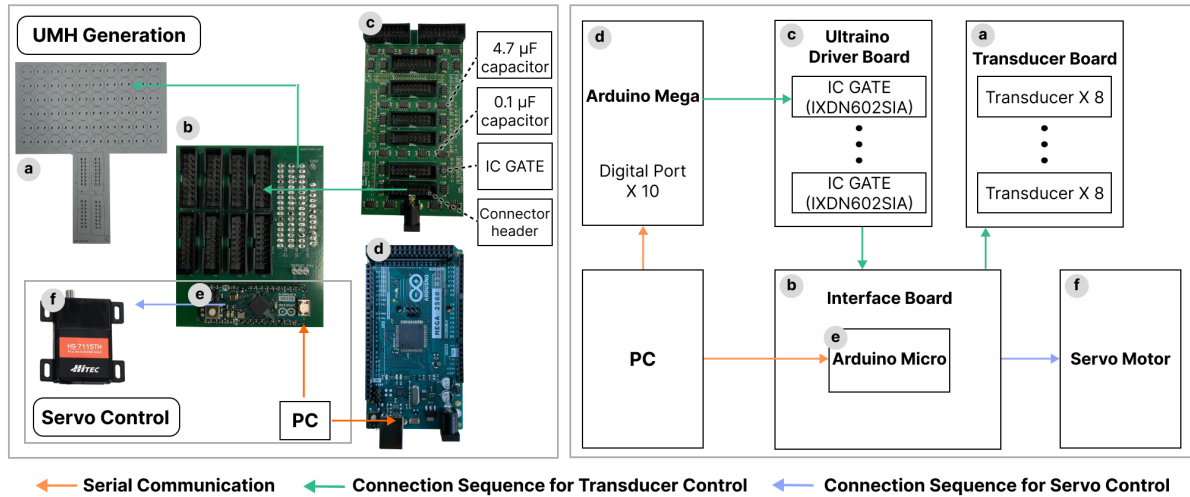


Fig. 3. Hardware overview. (a) A transducer board for mounting ultrasonic transducers, (b) an interface board that transmits signals from two MCUs to the servo motor and transducers, (c) a modified Ultraino driver board [54], (d) Arduino Mega that creates driving signals for UMH, (e) Arduino Micro that generates driving signals for servo motor, and (f) servo motor.

The first challenge lies in the device minimization. For a wearable form factor, reducing both size and weight is inevitable. The commercially available UMH device (Ultrahaptics STRATOS Explore [88, 95]) weighs 700 g, which makes it hard to be deployed for wearable applications. Also, it is required to generate focal points smaller than the surface area of the fingertips to deliver appropriate feedback. To address this, we simulated the spatial distribution of acoustic radiation pressure generated by ultrasonic transducer arrays of various shapes and sizes (See Section 4.2.1 and Section 4.2.2). This allowed us to identify an effective phased array design while minimizing array size, which is capable of providing haptic feedback across the entire hand.

The second challenge involves maintaining an effective distance range between the feedback point and the phased array. If the distance is too large, the attenuation effect of acoustic waves reduces the feedback intensity. In contrast, if the distance is too short, the directivity of the transducers limits their capability to generate full-powered haptic feedback. To address this issue, we simulated the spatial distribution of pressure generated at varying distances between the array and the focal point for the selected array shape (See Section 4.2.3). Based on the simulation results, we identified an effective range and proposed an algorithm and system that effectively delivers UMH feedback across the entire hand while maintaining this distance range.

The final challenge is the lack of knowledge on the perceptible intensity of UMH for the fingers. Prior UMH perception studies targeting the hand have been limited to the palm [19, 85, 94]. Although Pan et al. [65] investigated UMH perception focusing on the fingertip, they employed a commercial ultrasonic array. Further research is required to explore both perception and array design for wearable UMH targeting the fingertips. Therefore, we carried out a perception study targeting the fingers using UMH (See Section 5) and implemented a finger-level wearable UMH interface and system based on these results.

3.1 Hardware

Ultraboard consists of two main components: a transducer array for generating haptic feedback and a servo motor for manipulating the array platform. To identify an array capable of generating a focal point with sufficient intensity and size while minimizing weight and size, we utilized acoustic pressure simulations (Section 4).

The simulation results confirmed that a rectangular transducer array consisting of 10 horizontal by 6 vertical transducers is the effective shape and size, effectively delivering perceivable tactile feedback to fingertips. We employed ultrasonic transducers (MA40S4S, MURATA), where the transducer's angular dispersion is 80° . To ensure all transducers in a row contribute to generating the focal point at maximum intensity, we set the minimum focal length (the distance between the focal point and the transducer array) to 120 mm ($= \frac{100}{\tan 40}$), as shown in Figure 5.

We developed three custom PCB boards as shown in Figure 3, including a transducer board for mounting transducers, an interface board for transmitting signals from two microcontroller units (MCUs) to the servo motor and transducer, and an Ultraino driver board [54] with a replaced IC gate.

We mounted the transducers on a transducer board, which is fixed to the transducer array socket. Then, we connected these transducers to a wrist-mounted interface board, which is ultimately linked to the modified Ultraino driver board via a flat ribbon cable. Ultraino driver board controls 64 channels with a rectangular wave at $\pi/5$ phase resolution, allowing individual transducer control with a $2.5 \mu\text{s}$ time resolution. To generate higher intensity ultrasound, we modified the IC gate (IXDN602SIA, Littelfuse Inc.) to operate in a wider voltage range. Instead of the original Ultrino driver board's 17 Vpp amplification, the signal is amplified to 35 Vpp, powered by an external supply. This modified Ultraino driver board is connected to an Arduino Mega loaded with the Ultraino DriverMega firmware. We attached an Arduino Micro to an interface board on the wrist, which controls a servo motor (HS-7115TH, Hitec) based on the haptic rendering algorithm that moves the array according to the positional relationship between the fingers and the transducer array. Since the servo motor operates within a range of $0\sim 150^\circ$, we mounted it at an angle of 45° relative to the arm, rather than parallel, to accommodate a wider wrist movement range (Figure 2).

We chose the motor with 39 N/cm torque capable of manipulating a 325 g transducer array. At maximum speed, it takes about 270 ms to travel from one end position to the other. Arduino Mega and Arduino Micro communicate with the PC via a serial connection. They receive control signals generated by the PC based on interaction data from an Oculus Quest 3 (connected through Oculus Link) and positional data from OptiTrack. In other words, the control signals are calculated using a haptic rendering algorithm in the PC and then transmitted to the servo motor and transducers.

We 3D-printed polylactic acid (PLA) based sockets that contain the transducer array and the PCB with the Arduino Micro. The transducer array socket weighs 120 g, and the socket containing the Arduino Micro-mounted PCB weighs 175 g. Including both sockets and the strap, the total wearable parts of the prototype weigh 295 g. We excluded the weights of the Arduino Mega and Ultraino driver board, as they will be optimized in future product development stages. Section 8 discusses methods for miniaturization and optimization.

We measured the power consumption of the entire device, including the transducer array and servo motor. For the transducer array, the subsequent perception study indicated that a minimum driving voltage of 16V is required to generate perceptible feedback. Under these conditions, the power consumption is 1.94W in the active state and 0.16W in standby. From our user study (Section 6), the average typing speed was 12.462 WPM with a Key Press Duration of 160 ms. Based on these results, the transducers remain active for approximately 160 ms per second. This corresponds to an estimated power consumption of 0.44 Wh. For the servo motor, assuming a 30% active state ratio based on a user study, the power consumption was calculated as 0.23 Wh. The total power consumption of 0.67 Wh accounts for 1.87 % of the 35.9 Wh Apple Vision Pro battery [2] and 3.45 % of the 19.44 Wh Oculus Quest 3 battery [56]. This indicates that in a typical typing scenario, both cases allow for more than 24 hours of usage, assuming that only Ultraboard is operated.

The haptic interface is attached to the wrist using a strap and is designed as a rotating wrist mount type compatible with action cameras. Therefore, this design allows rotation along three axes to accommodate different users (Figure 2). We designed our prototype to avoid placing bulky equipment on the hand where we positioned the prototype on the inner wrist to prevent hand-tracking occlusion issues. Moreover, we employed a servo motor

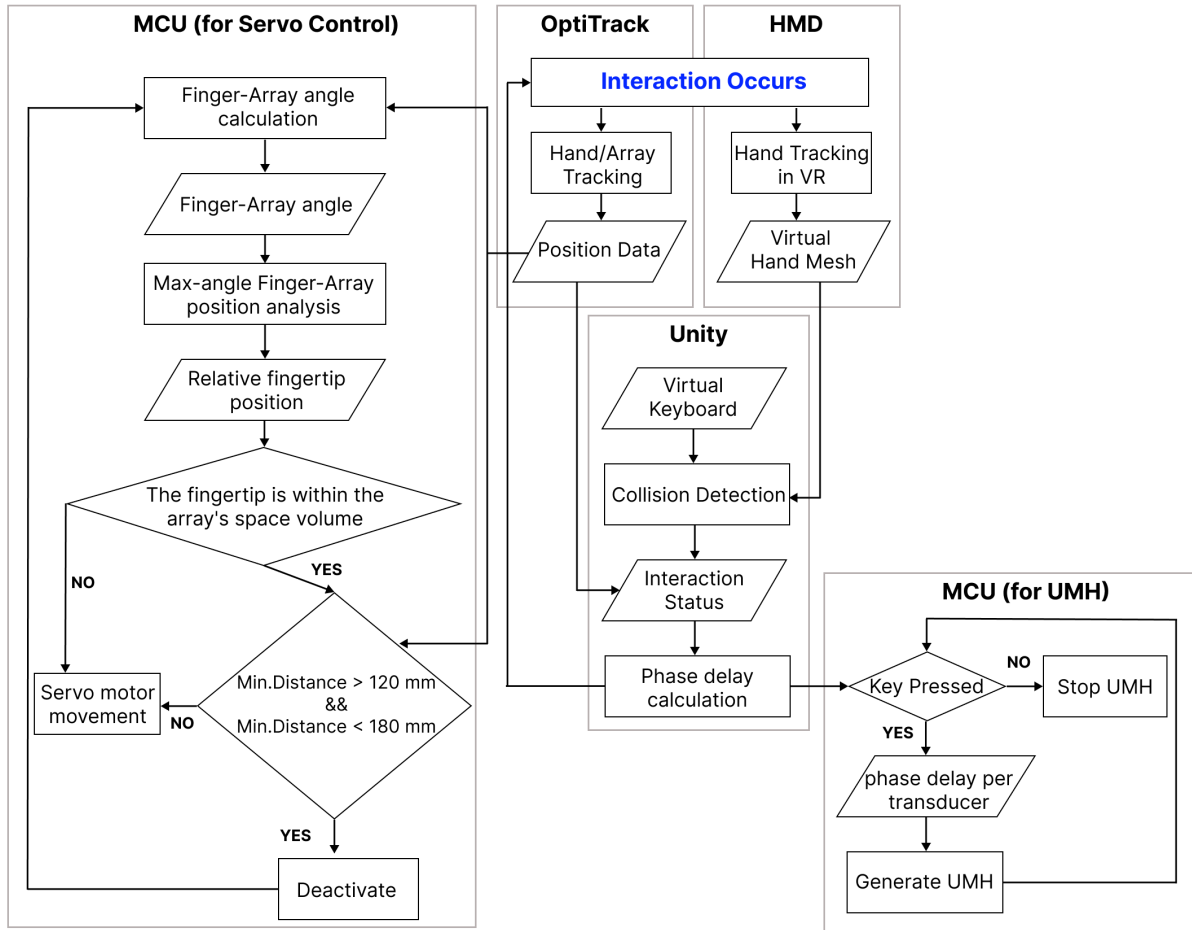


Fig. 4. Ultraboard haptic rendering pipeline and system overview. We employed HMD and OptiTrack to accurately track hands and a transducer array to support mid-air haptic rendering for VR typing.

to make the prototype available only when needed by activating the servo motor to place the transducer array in position. In this way, we minimized the interference with natural hand movement in our proposed wearable haptic interface.

3.2 Haptic Rendering Algorithm and Pipeline

To enable high degrees of freedom in hand-based interactions within VR environments, the array's position should be adjustable according to the hand's location in real-time, regardless of hand movement or wrist orientation. This adjustment ensures that the array is directed toward the focal point while maintaining a consistent focal length. To accomplish this, we developed a haptic rendering algorithm that controls servo motors based on real-time position data of the hand and array, enabling consistent UMH experiences (Appendix [Appendix A](#)). Figure 4

provides an overview of the haptic rendering pipeline. Real-time coordinates for each fingertip, hand, and the four vertices of the array are acquired using OptiTrack (NaturalPoint, Inc. [61]), while the HMD's hand-tracking feature detects interactions with virtual objects in the VR environment. When hand interaction begins, the haptic interface rendering algorithm is activated, initializing the servo motors to 120° to position the transducer array in its default orientation.

The servo motor control part of the haptic rendering algorithm operates in two main phases. In the first phase, the system uses OptiTrack data to assess the spatial relationship between the array and the fingertips of each frame. For each fingertip position P_{thumb} through P_{pinky} , each vector \vec{V}_{thumb} through \vec{V}_{pinky} is calculated, which is perpendicular to an imaginary line extending from the transducer array's center and parallel to its upper edge. The angle is then computed by taking the dot product between each \vec{V} and the array's normal vector \vec{N} . This angle refers to the 'Finger-Array Angle' shown in Figure 4. The array is then rotated so that the fingertip with the largest angle is positioned within its spatial volume. When the fingertip with the largest angle is outside the array's spatial volume, the servo motor adjusts the array position until it is within this volume. The second phase begins once the fingertips are inside the array's spatial volume. The system calculates the distance between each fingertip and the array, rotating the array to ensure that the minimum distance between the fingers and the array remains within the specified range (120 mm to 180 mm). This range was determined based on the directivity of the transducers (Section 3.1) and simulation results (Section 4). This process repeats continuously during operation, maintaining the position of the transducer array to ensure the delivery of consistently perceivable and effective feedback intensity.

4 TECHNICAL EXPERIMENT ON ULTRASONIC MID-AIR HAPTICS

In this section, we explore the spatial distribution to determine whether ultrasonic mid-air haptics are suitable for providing feedback to the fingers, while also investigating the appropriate shape and size of the transducer array and determining the effective focal length for the selected array. First, we present the technical principles of UMH. Then, we propose interface design guidelines suitable for finger-level wearable UMH based on simulations.

4.1 Ultrasonic Phased Array Operating Principle

To calculate the acoustic pressure field in three-dimensional space, we used the linear acoustics model, which is the basic model used to describe the propagation of sound waves. It is based on modeling theory widely used in the field of ultrasonic imaging and is very simple and accurate because it does not take into account the non-linear properties of acoustics [13]. In an array of multiple ultrasonic transducers, the superposition of the spherical waves emitted by each source transducer is described by Huygens' principle of the superposition [12, 54]. Therefore, the intensity of the acoustic pressure at a particular point (x, y, z) is the sum of the acoustic pressures at each transducer. The acoustic pressure at each transducer is as follows :

$$P(r) = P_0 A \frac{D_f(\theta)}{d} e^{i(\varphi + kd)} \quad (1)$$

As depicted in the figure 5, P_0 represents the constant for the amplitude power of the transducer. A indicates the peak-to-peak amplitude of the driving signal. D_f refers to the far-field directivity function and φ is initial phase. The term k denotes the wave number, while d stands for the distance between the transducer and focal point, meaning the propagation distance [12, 54]. Equation 1 is mainly composed of a directivity function, which describes how the intensity of the energy radiated in space changes with direction, and a phase delay, which takes into account the distance between each transducer and the focal point. Considering the mechanical aspects of the transducer, for a flat circular piston source (transducer), the directivity function for modeling the distribution of pressure is $D_f = 2J_1(ka \sin \theta) / ka \sin \theta$. J_1 is a first-order Bessel function of the first kind and θ represents

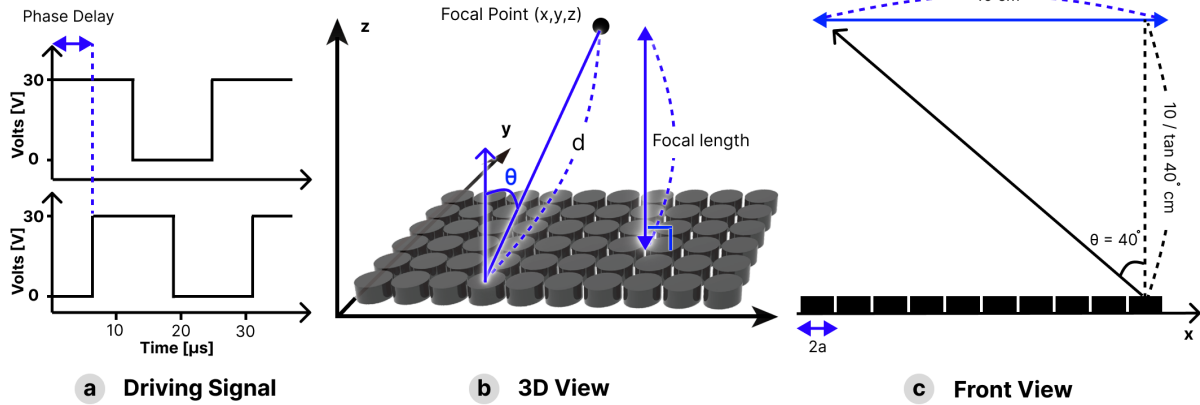


Fig. 5. Ultrasonic mid-air haptic operating principle. (a) Each graph illustrates an example of a transducer driving signal with a duty cycle of 50 % and a driving voltage of 30V. The upper graph represents the initial phase, while the lower graph shows a phase delay of 0.25π . (b) 3D View of the acoustic pressure field. It represents the parameters for calculating acoustic pressure. (c) Front view of the acoustic pressure field. It represents the minimum focal length at which all transducers in a row can contribute to generating the focal point, taking into account the directivity of each transducer.

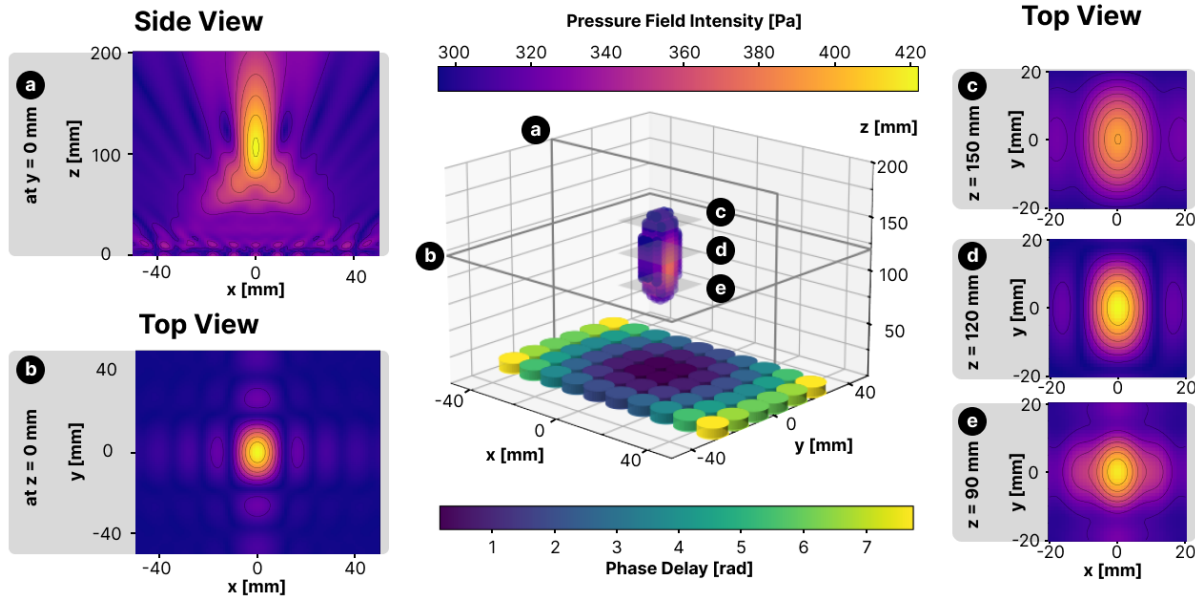


Fig. 6. Simulated spatial distribution cross-section of acoustic pressure at $y = 0$ mm and $z = 120$ mm (Left). Simulation of the focal region corresponding to 70% of the maximum acoustic pressure intensity and the phase delay per transducer (Center). Simulation of the XY cross-sections at $z = 150$ mm, 120 mm, 90 mm (Right).

the angle between the transducer’s normal vector and the line connecting the transducer to the target point. a denotes the radius of the transducer [13].

Also, previous UMH researches have demonstrated that direct acoustic radiation pressure at the focal point is the primary source of haptic feedback, with little consideration of acoustic effects from reflections [33]. This suggests that the energy density of reflected ultrasound is relatively low and negligible. Therefore, we infer that the multi-path effect does not significantly affect the performance of our wearable form factor system.

4.2 Simulation for UltraBoard Phased Array Design

Drinkwater et al. demonstrated that acoustic pressure simulations based on a linear acoustic model show a deviation of less than 20 % compared to actual measurements [12]. Therefore, in this section, we simulated acoustic radiation pressure to explore the effective phased array configuration. Figure 6 presents an example simulation result illustrating the 3D distribution of acoustic radiation pressure generated by the phased array. Center shows the iso-contour at 70% maximum of the focal region calculated when the position of the focal point is set to (0,0,12). The transducers are located at $z=0$, and each color represents the phase delay of the corresponding transducer. (a) and (b) shows the cross-section at $z = 120$ mm and $y = 0$ mm respectively. Additionally, (c), (d), and (e) show the XY cross-sections at $z = 150$ mm, 120 mm, 90 mm, respectively. First, we compared simulation results for different phased array shapes to determine the effective shape. Next, we compared the results based on the phased array's size to identify the effective size. Subsequently, we evaluated the acoustic pressure generated at various focal lengths to determine the maximum focal length and define the range of focal lengths that should

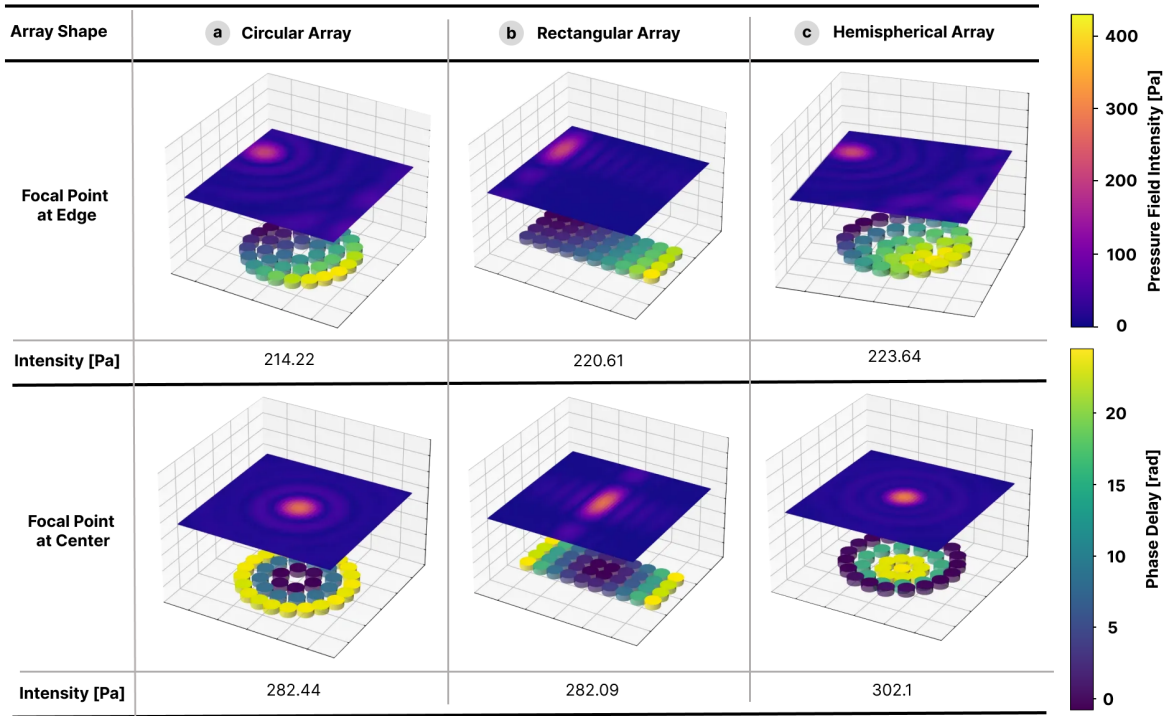


Fig. 7. Simulated intensities and spatial distribution cross-sections of acoustic pressure at $z = 120$ mm and phase delay per transducer for three phased array shapes (a) Circular Array (b) Rectangular Array (c) Hemispherical Array, with the focal point set at the center and at the edge.

be maintained in our system. Finally, we compared the simulated and measured pressure intensities to verify whether the feedback generated at the edges is suitable for finger-level haptic feedback.

4.2.1 Simulation for phased array shape. We compared simulation results for three different shapes to identify a suitable phased array shape: circular, rectangular, and hemispherical. To account for usability and hand width (average adult male hand width of 104 mm [87]), the phased array's width was set to approximately 10 mm. The number of transducers in each array was standardized to 40 in the simulation for shape. Figure 7 showed that when the focal point was positioned at the center of the array, the circular and rectangular arrays produced similar intensities at the center. However, the rectangular array generated stronger acoustic pressure at the edges.

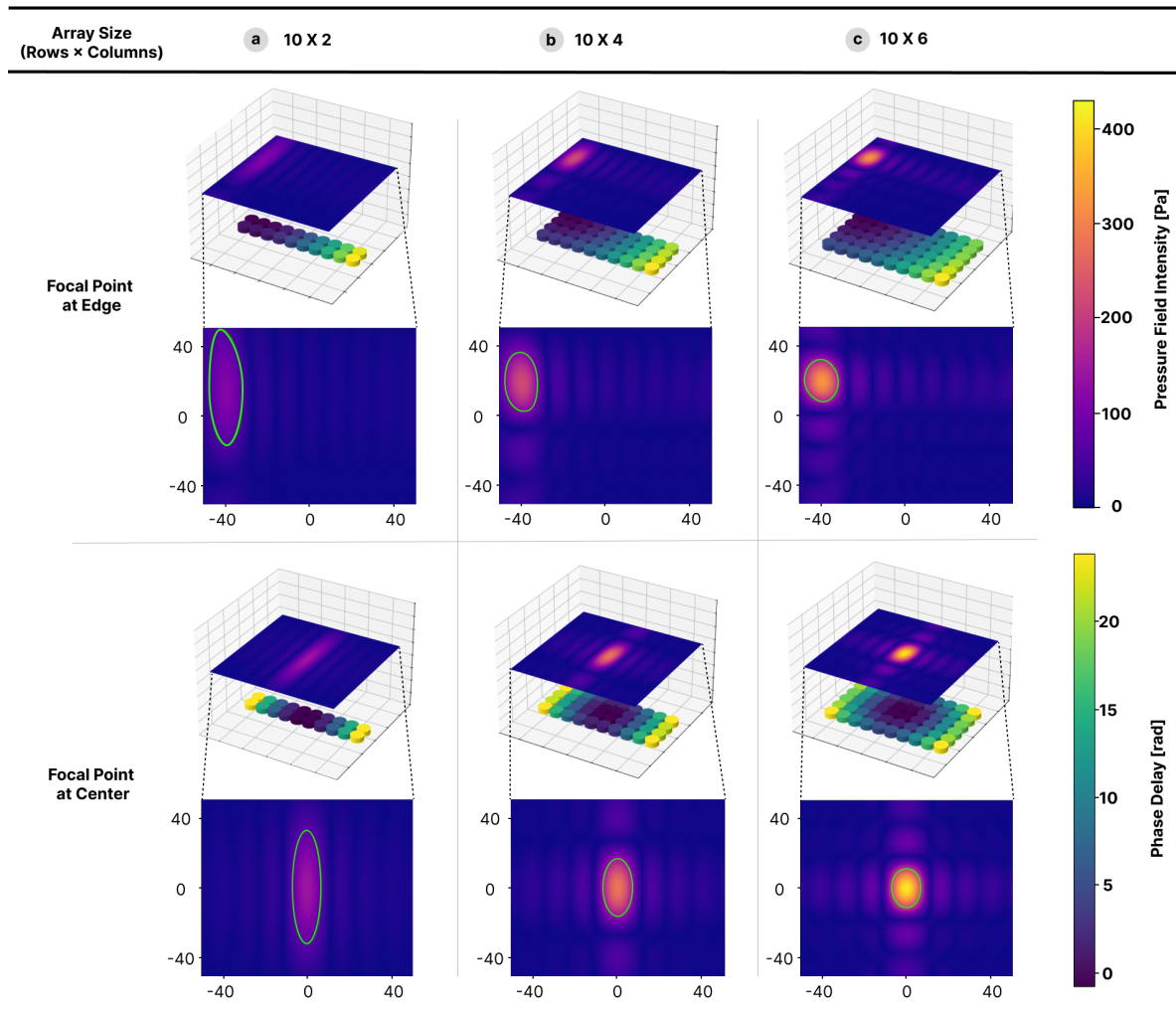


Fig. 8. Simulated spatial distribution cross-sections of acoustic pressure at $z = 120$ mm and phase delay per transducer for three phased array sizes (a) 10×2 (b) 10×4 (c) 10×6 (the number of transducers), with the focal point set at the center and at the edge. The green lines indicate 50% of the maximum intensity.

While the hemispherical array produced about 7.1 % stronger acoustic pressure compared to the rectangular array, its volume increased by approximately 80 %. Considering both comfort and wearability, as well as the need to minimize interference with the user's movements, we ultimately selected the rectangular array, which balances performance and compactness.

4.2.2 Simulation for phased array size. Then, we compared the focal regions generated by three different array configurations: 2×10 , 4×10 , 6×10 with the focal point positioned at the center (0,0) and the edge (-40,20) at $z = 120$ mm. Figure 8 shows simulation results of the focal point generated by each phased array, with the green line (focal region boundary) covered area illustrating 50% of the maximum intensity. For the (a) 2×10 and (b) 4×10 arrays, the focal points are not small enough (60 mm and 40 mm respectively) to provide feedback to the fingertip. A large array of transducers and a short focal length are required to produce a small focal point, and the pressure tends to increase as the number of transducers increases [12]. To enhance interaction performance by providing tactile sensation, it is necessary to provide as strong a tactile sensation as possible and generate a compact focal point that does not exceed the area of a finger. Therefore, we chose a 6×10 phased array design that offers the most compact focal point and strongest intensity.

4.2.3 Simulation for focal length. In this section, we conducted simulations to determine the appropriate range of focal length for generating finger-level haptic feedback (Figure 15 in Appendix Appendix B). Based on the results from previous simulations, we simulated with a rectangular array consisting of 60 transducers. As the focal length increases, the acoustic radiation pressure attenuates, resulting in a weaker intensity. When the focal length reaches 200 mm and the focal point is positioned at the edge of the phased array, the maximum intensity of the main lobe is 248.8 Pa, while the maximum intensity of the side lobe is 183.6 Pa, corresponding to 74 % of the main lobe. This causes the feedback to be perceived not as a single point on the finger but as a broader area across multiple fingers. From these results, we set the focal length range with a maximum of 180 mm and a minimum of 120 mm, determined by the mechanical properties of the transducers (Section 3.1). To maintain the focal length within this range, we developed an algorithm that dynamically rotates the phased array.

4.2.4 Center vs. Off-Center. In order to provide adequate feedback to various parts of the user's hand, the phased array must be able to provide feedback above a threshold that is perceived by the user, not only at the center of the phased array but also at the edges. To demonstrate this, a total of 6 points were selected as focal points at a focal length of 120 mm, including the center and edge, due to the symmetry of the phased array shape. We measured the acoustic radiation pressure at these points at maximum voltage (30 V). Figure 9 shows a system

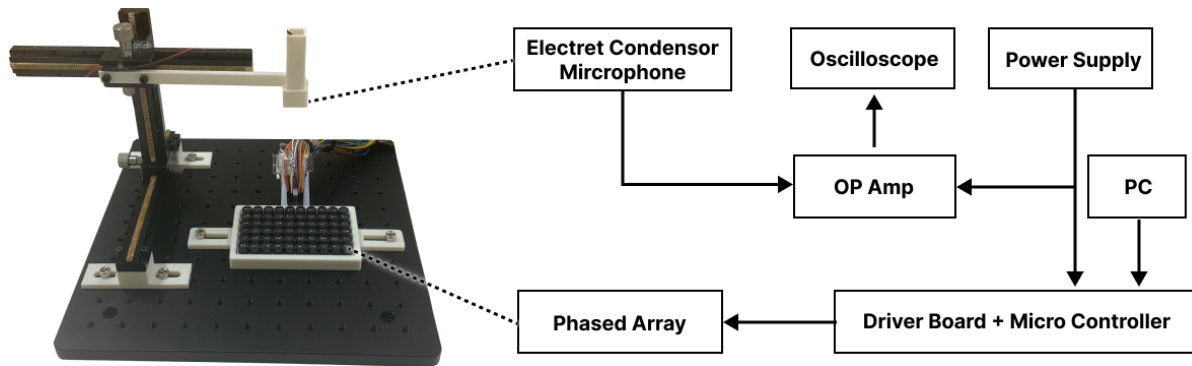


Fig. 9. Experimental setup for acoustic radiation pressure measurements.

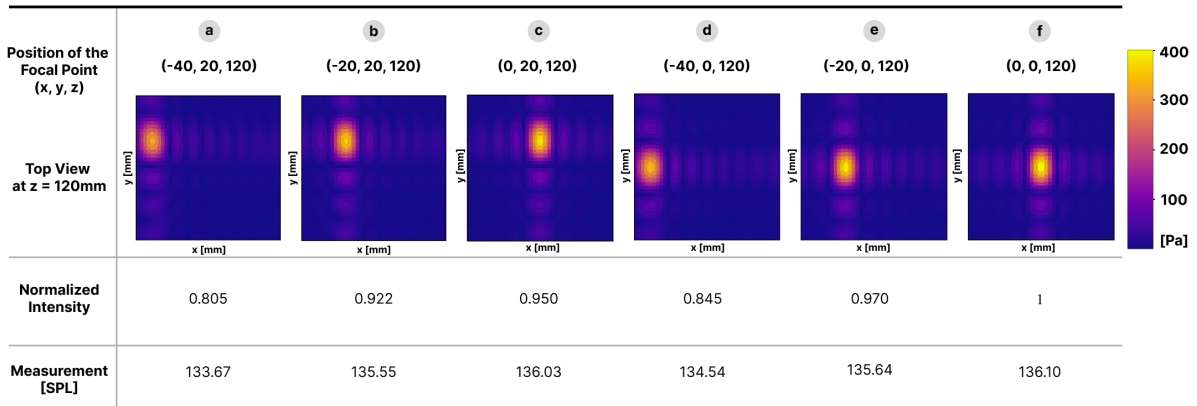


Fig. 10. For a hphased array size of 10×6 , simulations were conducted for the spatial distribution cross-section of acoustic pressure at $z = 120$ mm with focal points (x, y, z) set at various locations (a~f). The results show the ratio to the maximum acoustic pressure intensity and the actual measured values.

overview of the measurement of the acoustic pressure. As shown on the left side of the figure, the phased array is fixed on the floor facing upward, and the electret condenser microphone is mounted on a 3D stage to measure the actual intensity of the generated acoustic radiation pressure. The aperture of the microphone is 4 mm.

The transducer driving signal generated by calculating the phase delay of each transducer on the PC is transmitted to the MCU and driver board via serial communication. For signal amplification, an operational amplifier (op-amp) circuit was connected to the microphone, and the acoustic radiation pressure output was observed through the FFT function of the oscilloscope.

Figure 10 shows the simulation results and measured values at each point.: a) 133.67dB SPL, b) 135.55dB SPL, c) 136.03dB SPL, d) 134.54dB SPL, e) 135.64dB SPL, and f) 136.10dB SPL. Since the sound pressure level is given by $L = 20 \times \log_{10} \left(\frac{P_1}{P_2} \right)$, the trend in intensity differences at each point matches between the actual measurements and the simulation results (e.g., a/f : simulation 0.805, measurement 0.794). As in the simulation, the acoustic pressure is generated weakest at the point most distant from the center of the phased array. Therefore, we conducted a subsequent perception study to identify the minimum perceivable intensity on the fingers and verified that the measured value at the phased array's edge exceeds this minimum intensity.

5 PILOT STUDY: PERCEPTION STUDY

As demonstrated in the previous section, research on the perception of UMH has primarily focused on the palm. To investigate the perception of UMH on the fingers, we conducted an experiment to examine how individuals' perception changes based on key parameters of UMH: *modulation frequency*, *feedback duration*, and *location*. By comparing the experiment results with the measurements from Section 4.2.4, we identified the minimum intensity threshold required to deliver perceivable feedback across all areas of the hand using the Ultraboard.

5.1 Study Parameters

5.1.1 Modulation Frequency. The glabrous skin, including the palm and fingertips, contains a variety of mechanoreceptors such as Merkel cells, Meissner's corpuscles, and Pacinian corpuscles. Humans detect various tactile sensations such as touch, pressure, and vibration through these mechanoreceptors. The distribution density of mechanoreceptors has a strong influence on tactile sensitivity, and Pacinian corpuscles play a large role in

vibration detection (~250 Hz) in the hand [41]. Humans are most sensitive to vibrations in the range of 150~250 Hz on the fingers and palm [72]. If UMH is generated using lateral modulation [85], feedback with a modulation frequency of approximately 50~200 Hz can be detected in the glabrous skin. Also, the sensitivity threshold gets smaller as the frequency increases within this range [30, 85]. To confirm that this tendency is also seen in the fingertip, a perception study was conducted for two modulation frequencies: 50 Hz and 200 Hz.

5.1.2 Feedback Location. Estimates of Pacinian corpuscles decrease with distance from the center of the body [11], which aligns with the fact that the center of the palm is more sensitive to UMH than the fingertips [82]. Kalantari et al. found that the index and middle fingers are sensitive to ultrasonic vibration, while the pinky finger is the most insensitive [42]. This is because the index and middle fingers have a high density of mechanoreceptors [41]. Therefore, to determine the minimum intensity of UMH feedback across the entire hand, including the fingers, we conducted a perception study focusing on the minimum intensity thresholds for the middle and pinky fingers.

5.1.3 Feedback Duration. Previous studies indicate that UMH feedback durations under 50 ms are challenging for individuals to perceive UMH feedback [71], while a duration of 200 ms is considered most suitable for brief interactions such as button clicks [64]. Wilson et al. compared durations of 100 ms and 1000 ms, finding that longer durations allowed users to more accurately localize the stimulus [94]. Rümelin et al. tested durations of 50 ms and 130 ms, finding no significant difference in perception between the two, both being adequate for brief feedback [71]. Accordingly, we set the feedback durations to 100 ms for relatively short feedback within a perceivable range and 500 ms for sufficiently long feedback in our experiment.

5.2 Setup

Figure 11 (b) illustrates the setup for our perception study where the phased array was positioned at the microphone location in Figure 9 facing the floor. The hand was placed on the floor with the palm facing upwards to minimize arm fatigue and maintain a constant focal length during the experiment.

The perception study was conducted with 25 participants (15 females, 10 males. Age of 21 to 31. SD=3.08). All participants were right-handed and experimented with their left hand. All but two participants had no previous experience with UMH. The experiment took approximately 2 hours, including a break between each session, and participants were paid \$20 for their participation.

Participants sat in front of the experimental setup and were given a brief description of the experiment and instructions. The thickness of the user's finger was measured, and the position of the phased array was adjusted before the start of each session to maintain a focal length of 120 mm for all users. Training sessions were then conducted as many times as the participant desired until they were comfortable and familiar with the UMH. Participants wore headsets with white noise playing to minimize auditory cues. We displayed only the instructions on the experimenter's screen to minimize visual distractions and focus on the haptic feedback. In this minimized distraction environment, participants focused solely on the sensation of their fingertips and responded to whether they felt the feedback or not.

The experiment was designed as a within-subject study. The study consisted of a total of 8 sessions, corresponding to the two levels of each of the three independent variables. To minimize user fatigue, the session order alternated between the two locations and was randomized across participants to avoid bias. Each session was conducted using a modified two-down/one-up double staircase method [48]. In the adaptive procedure, the ascending staircase and descending staircase were conducted simultaneously and counterbalanced in order to prevent participants from making predictions. The ascending staircase started at 7 V and the descending staircase started at 31 V. The intensity of the UMH generated was controlled by manipulating the input voltage manually. In each staircase, the step size before the three reversals is 3 V, and the step size afterward is half of 1.5 V. The average of the last 6 reversal point values was used to estimate the resulting threshold. (Fig 11 (a))

5.3 Results

A 3-way ANOVA and post-hoc comparison showed that there was no significant difference based on feedback location. However, feedback duration had a statistically significant effect on the perceivable minimum intensity threshold. Feedback with a duration of 500 ms showed a significantly lower perceivable threshold compared to 100 ms feedback. ($p < 0.001$) Modulation Frequency also showed a significant increase for 50 Hz over 200 Hz, except for the feedback duration of 100 ms. ($p < 0.05$) The experimental results are consistent with previous findings, showing that longer feedback durations and frequencies between 150~250 Hz are easier to perceive. Although feedback location did not show statistical significance, we designed Ultraboard to provide UMH feedback to all ten fingertips because they have similar thresholds regardless of the sensitivity of each finger as shown in Figure 11 (c). In addition, we set the modulation frequency of UMH to 200 Hz for interactions with Ultraboard, as

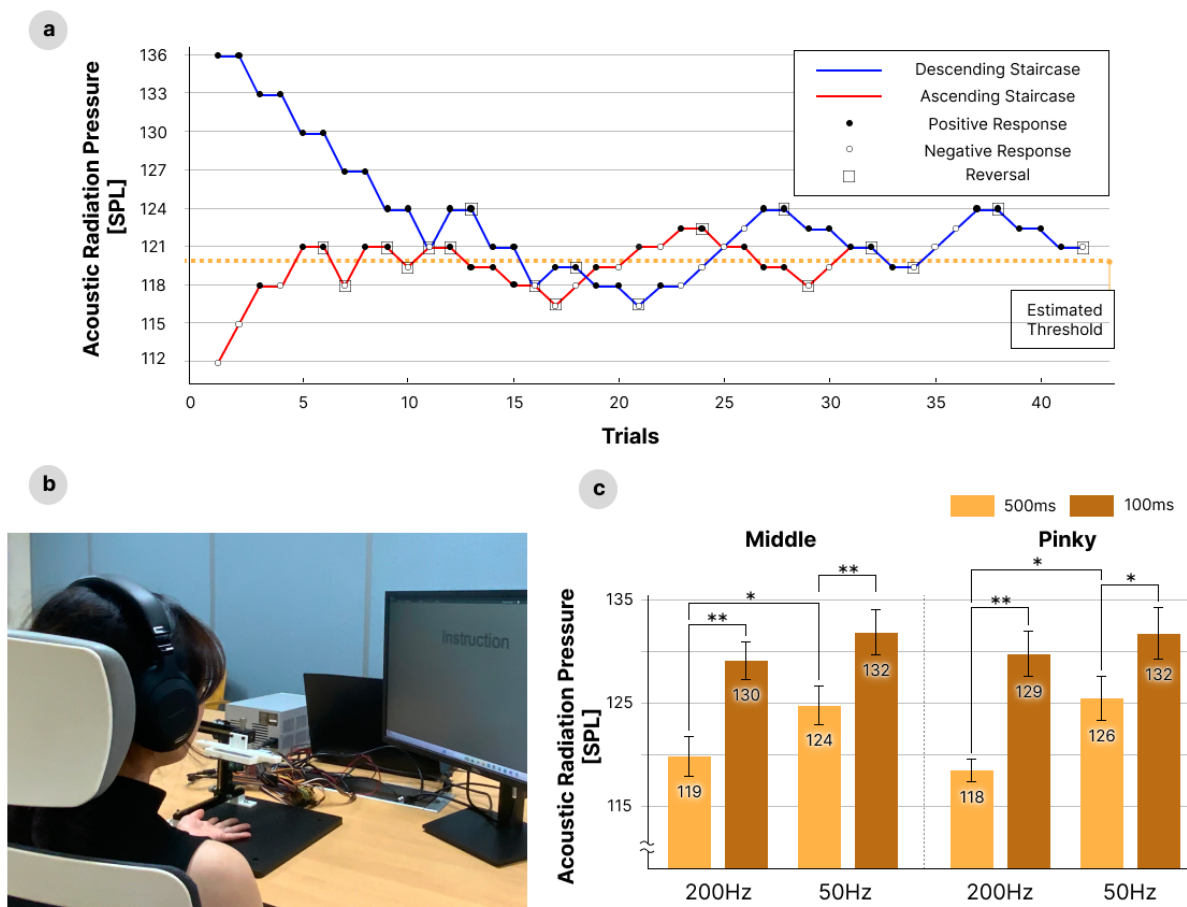


Fig. 11. Result and setup of the perception study. (a) An exemplary result of the adaptive procedure from one of the participants. (b) The experimental setup of the perception study. (c) Minimum perceivable acoustic radiation pressure intensity threshold for types of UMH by parameters. *, ** denotes significance level of $p < .05$, $p < .001$. Error bars denote 95% confidence intervals.



Fig. 12. User study setup. (a) Visualization of the position data of the fingers, palm, and vertex of the phased array obtained via OptiTrack, along with the phased array. Transducers with the same phase delay are assigned identical arbitrary colors. (b) A virtual environment scene showing a virtual keyboard and virtual hands during the user study. (c) The real scene of the experimental setup with a participant. OptiTrack markers are attached to the fingertips, the back of the hand, and the four corners of the phased array.

it has a relatively lower threshold. Additionally considering the experimental results depending on the feedback duration, we implemented interactions using feedback with an intensity greater than the minimum threshold intensity for each duration. And these results can be used as design guidelines for UMH feedback parameters targeting the fingers.

6 USER STUDY

In this user study, we investigated the impact of Ultraboard on both objective and subjective performance compared to conventional VR typing, only providing visual feedback. To assess common and essential interactions, we selected a VR typing scenario. For objective measures, we evaluated typing speed, key-press duration, inter-key intervals, and error rate. In addition, we measured the time taken to correct a typo to assess the performance using haptic feedback enabled by Ultraboard. For subjective evaluation, we examined user experience feedback related to typing. Through this study, we observed the effectiveness of Ultraboard in typing scenes and identified its potential for further development as a versatile and general-purpose haptic feedback interaction.

6.1 Setup

We recruited 24 participants (12 females, 12 males. Age of 22 to 34. $SD = 3.14$). All participants were newly recruited to avoid overlap with those in the Perception Study (Section 5.2), and they had no issues wearing the prototype and HMD or perceiving tactile sensations. Except for two participants who regularly used VR for typing and three who had some prior experience, the remaining 19 participants had no experience typing in VR. Additionally, all but one participant had never experienced UMH.

In this study, participants were asked to transcribe phrases displayed in front of them as quickly and accurately as possible using a virtual keyboard and virtual hand (Figure 12). We designed a virtual QWERTY keyboard with 26 alphabet keys and 3 control keys (space, backspace, enter). To prevent the keyboard UI from affecting the results, the design is based on Meta's Virtual Keyboard [55], which users can commonly use in commercial VR systems. The total keyboard area is $1516 \text{ px} \times 700 \text{ px}$. Each alphabet key is $115 \text{ px} \times 115 \text{ px}$ square and separated by 20 px. The widths of the spacebar, enter key, and backspace key were set to 5 times, 1.5 times, and the same width as an alphabet key, respectively. Before each experiment, participants were allowed to adjust the keyboard's position to their comfort, just like in usual VR applications.

To examine the effect of Ultraboard's haptic feedback, we conducted a within-subject study across three conditions: only visual feedback (V), only haptic feedback (H), and both visual and haptic feedback (VH). The 'V' condition served as the baseline, where the color of the pressed key changed to red during typing. In the

'H' condition, no visual change occurred, but haptic feedback was provided to the fingertip pressing the key. Lastly, in the 'VH' condition, the key color changed while haptic feedback was also delivered to the pressing fingertip. Additionally, we introduced a novel typo-correction interaction for VR typing. Here, we provided brief and rapid UMH feedback (200 Hz, 200 ms) to the right palm when a typo occurs. This quick and intense feedback is well-suited for typo alerts as it elicits an immediate and strong sensory response [60]. This feedback was provided in the 'H' and 'VH' conditions. For all conditions, the entered text appeared below the target phrase.

The order of conditions was counterbalanced across participants. Each condition involved the transcription of 10 unique phrases, with an additional 5 phrases used for practice before each condition. Phrases were randomly selected from the MacKenzie phrase set [52] without repetition across conditions. The entire experiment took approximately 2 hours per participant, and the participants wore noise-canceling headphones to block any auditory cues.

6.2 Procedure

After completing the consent form and receiving brief instructions, participants completed a short survey about their prior VR typing and UMH experiences before beginning the experiment. Participants then put on the prototype, HMD, and headphones. We asked participants to wear the armband as tightly as possible to prevent unintentional axial rotation caused by user movements. Prior to each condition test, they typed five practice phrases to familiarize themselves with the feedback, initiating the test by pressing the enter key once training was complete. After each phrase, participants pressed enter to proceed to the next one. Once all 10 phrases were transcribed, the condition test concluded, and participants provided subjective ratings on their typing experience. Participants took 5-minute breaks between each condition to relieve arm and hand fatigue. After completing all condition tests, participants provided feedback on their experience with the prototype and the typing task.

6.3 Results

6.3.1 Quantitative Results. A repeated measures ANOVA and a pairwise Tukey test were conducted across the three conditions (V, H, VH). Consistent with previous research that haptic feedback does not affect typing speed [25, 26], the presence of haptic feedback alone did not have a significant effect on typing speed (WPM) between the 'V' and 'VH' conditions. Dube et al. provided mid-air haptic feedback for keyboard presses and reported that, unlike previous research and our user study results, feedback influenced typing speed [14]. We speculate that this discrepancy is due to differences in feedback intensity resulting from variations in form factor size. In their study, haptic feedback was generated using the Ultrahaptics STRATOS Explore [88], consisting of 256 ultrasonic transducers, whereas we minimized the phased array size to accommodate a wearable form factor. However, a statistically significant difference in speed was observed between the 'H' and 'VH' conditions, suggesting that visual feedback, rather than tactile sensation, primarily influences typing speed ($p < .05$) in VR typing. Specifically, we performed a Friedman test to examine differences in Inter-Key Interval (IKI) and Key Press Duration (KPD) among the three conditions. However, the results did not show statistically significant differences. We also performed a Friedman test and post-hoc comparison to assess the impact of the typo-correction interaction which creates haptic feedback on the palm upon typo detection. Here, we observed a significant difference between the 'V' and 'VH' conditions ($p < .05$). This indicates a significant impact on user experience from the typo-correction interaction enabled by Ultraboard.

Similarly, a Friedman test was conducted to examine the effect of haptic feedback on error rates across the three conditions. The presence of haptic feedback did not have a statistically significant impact on error rates (Total error rate and uncorrected error rate). We assume that this is because the accuracy of hand tracking and the stability of hand visualization within the HMD primarily influence typing accuracy, while haptic feedback has little impact on typing precision.

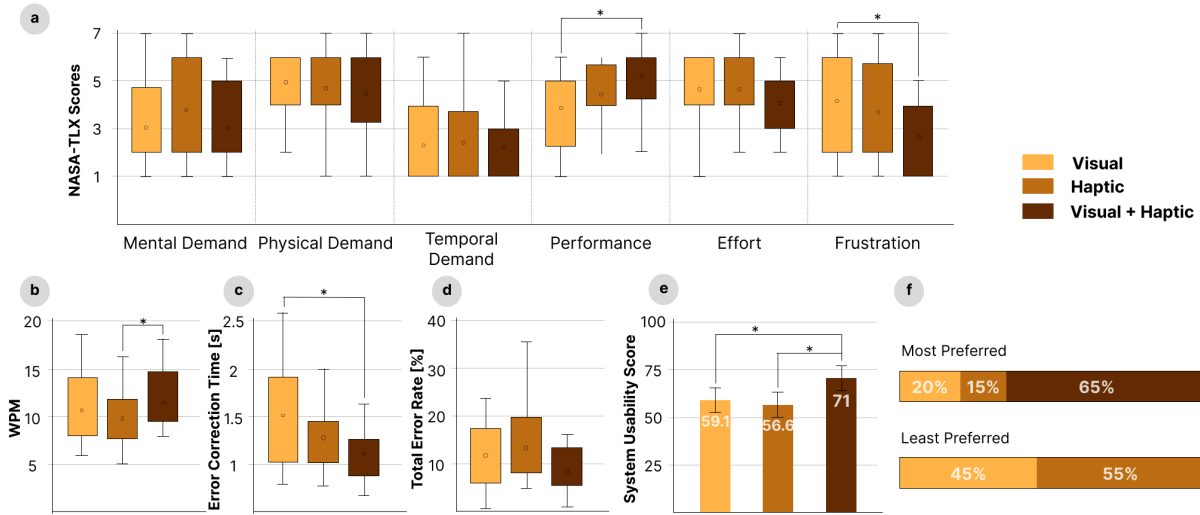


Fig. 13. User study results include (a) NASA-TLX rating for each condition, (b) typing speed, (c) time taken for typo correction, (d) total error rate, (e) system usability score for each condition, and (f) feedback preference survey results. Error bars denote 95% confidence intervals. * denotes significance level of $p < .05$.

After each condition test, we asked participants 16 questions related to usability and workload to obtain subjective ratings (6 NASA-TLX questions [28], 10 System Usability Scale questions [62]). At the end of the experiment, a post-interview was conducted to gather qualitative feedback from participants.

6.3.2 Qualitative Results. We conducted a One-way ANOVA to assess the impact of each condition on cognitive and physical task load. No statistically significant differences were observed between conditions for mental, physical, or temporal demand, as well as for effort. However, Tukey’s post-hoc test indicated significant differences between the ‘V’ and ‘VH’ conditions for confidence and frustration ($p = 0.009 < 0.05$, $p = 0.029 < 0.025$, respectively), as depicted in Figure 13 (a). We assume that the significant improvement in confidence and frustration with the addition of haptic feedback is due to the clear completion cue it provides for each key press. In contrast, the lack of improvement in demand and effort appears to reflect a trade-off between the benefits of feedback and the additional effort and fatigue from wearing the equipment.

To evaluate usability across each condition, we conducted a One-way ANOVA and Tukey test on the System Usability Scale (SUS) scores. Statistically significant differences were found between the ‘H’ and ‘VH’ conditions ($p = .006 < 0.05$) and between the ‘V’ and ‘VH’ conditions ($p = .028 < 0.05$), as depicted in Figure 13 (e). These results indicate that both visual and haptic feedback contributes to user experience, and usability is enhanced when both types of feedback are provided together.

In the short interview conducted after the experiment, 17 participants (65%) indicated a preference for the ‘VH’ feedback among the three feedback types, while 4 participants (20%) preferred ‘V’, and 3 participants (15%) preferred ‘H’. Participants cited the weight of the interface and the artificial tactile sensation, which differs from actual typing, as reasons for their preferences. Although participants noted that the presence of haptic feedback helped confirm typing completion and enhanced a sense of immersion, the weight-induced fatigue appeared to influence preference differences. Conversely, when asked about the least preferred feedback, 11 participants (55%) selected ‘H’, and 13 participants (45%) selected ‘V’, with no participants selecting ‘VH’ as the least preferred.

Furthermore, we conducted a 7-point Likert scale survey in a short interview to assess comfort both with and without the device. The mean comfort rating was 3.25 for Bare hands and 3.9 for Ultraboard, while the difference was not statistically significant. It is noteworthy that there was no statistically significant decrease in the scores. Additionally, when asked, "Would you be willing to use Ultraboard despite the additional weight burden?" 70 % of participants responded that they would be willing to use the device. Feedback such as "*The feedback provided to individual fingers during typing was beneficial from a perceptual perspective,*" along with improved scores in the confidence and frustration categories of the NASA-TLX results, suggests that Ultraboard effectively reduced visual load. Despite the need to wear additional equipment, these findings indicate a high level of user preference. We can infer that the user fatigue and comfort associated with the additional weight burden of Ultraboard remain within an acceptable range.

7 USE CASE SCENARIO

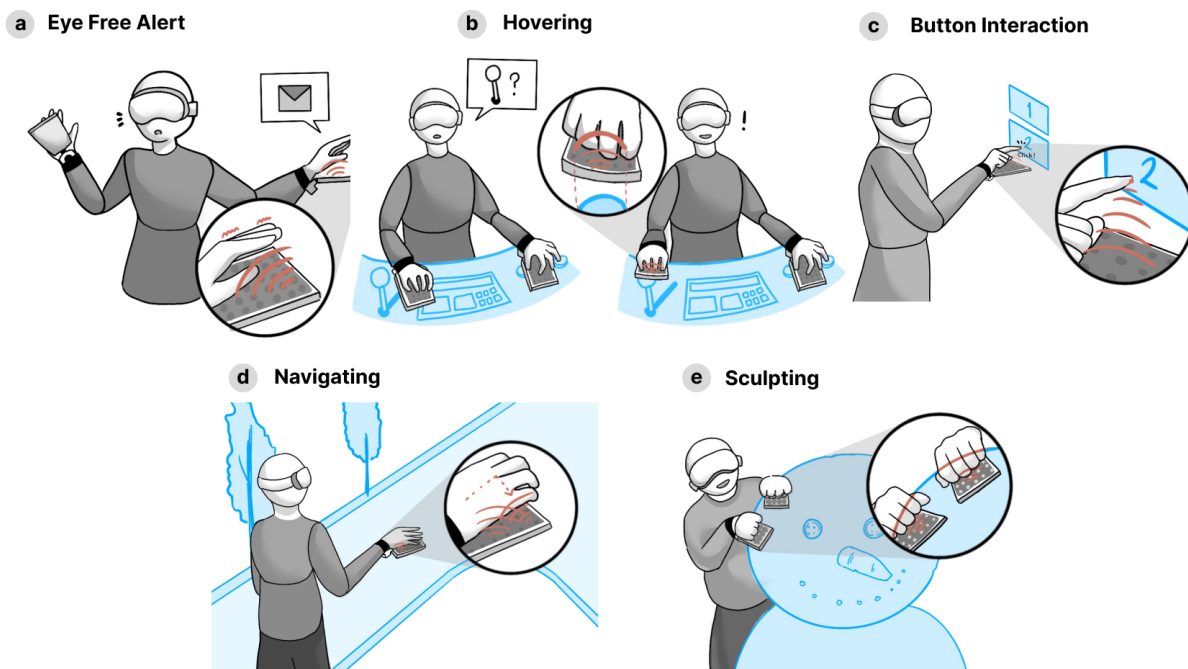


Fig. 14. Use case scenarios include (a) alert, (b) hovering without visual focus, (c) button click feedback, (d) directional information, and (e) feedback for large objects without workspace limits.

Ultraboard provides UMH feedback with sufficient intensity and precision to effectively target the fingertips, making it well-suited for applications where fingers are the primary interaction tool. While VR typing was selected as a fundamental VR interaction for the user study, Ultraboard's ability to deliver consistent feedback without being constrained by hand movement or location broadens its applicability across diverse use cases. Ultraboard can be utilized in a wide range of VR applications, and we propose use cases such as eyes-free alerts, button interactions, hovering, navigating, and sculpting. (Figure 14)

Eyes-free Alerts In current VR systems, alerts are typically provided to users through visual cues within the HMD display or by utilizing vibrations in the controller. However, these solutions disrupt user immersion due to

visual distractions or require a user to constantly hold the controller [10]. On the other hand, Ultraboard delivers alerts outside the HMD's field of view, regardless of the user's posture.

Button Interactions Button interactions, a type of VR typing tested in our user study, are essential in VR environments. Current VR systems rely on simple visual cues for button input, but Ultraboard enables the simulation of button stiffness and provides tactile sensations [38, 53]. Accordingly, Ultraboard delivers multimodal sensations that allow buttons to be perceived in various forms by adjusting UMH intensity and parameters according to user preferences. Its ability to provide consistent feedback regardless of button location makes Ultraboard well-suited for button interaction in VR.

Hovering In VR environments, interacting with specific UI elements or grasping virtual objects requires users to visually confirm the location and move their hands accurately. It often leads to unnecessary head movements, causing eye and neck strain. For frequently used objects, such as directional keys or controllers, providing a tactile sensation to the fingers or palm when the hand reaches the correct position allows users to interact with the objects without disrupting their focus.

Navigating UMH can represent not only static focal points but also multi-focal points and dynamic strokes by shifting focal points, enabling the expression of various shapes and movements [50]. Therefore, Ultraboard can be utilized in navigation tasks to provide directional guidance along a path. Furthermore, Ultraboard supports a large workspace and flexible wrist movement, enabling users to receive directional information while moving their arm and hand naturally.

Sculpting Previous research on haptic devices has explored combining haptic and visual feedback in VR environments [86]. However, these devices restrict user movement or are limited by their size, making it challenging to handle large workspace volumes and interact with large virtual objects. In contrast, Ultraboard is a wearable phased array that can be repositioned in real time to the ideal location, allowing it to provide consistent haptic feedback regardless of user movement or position. This capability makes Ultraboard suitable for interactions involving large objects, such as sculpting.

8 DISCUSSION

Ultraboard offers the following advantages. First, the minimized prototype, compared to traditional UMH interfaces that occupy relatively large spaces, enhances usability and applicability. Second, Ultraboard can operate as a mid-air wearable device without spatial constraints like user movement. Third, an algorithm for repositioning the phased array enables always-available perceptible feedback across the entire hand. Lastly, the use of UMH technology brings dynamic and active feedback rather than passive feedback. Therefore, Ultraboard promotes always-available and effective interactions compared to using rotatable physical keyboards, which are limited to providing only passive feedback. Moreover, the approach of simply using a rotatable physical keyboard not only requires additional force to support key presses but also has the limitation that the feedback area is constrained by the size of the keyboard.

There also exist limitations. Despite minimizing the phased array, the current prototype weighed 295 g, which may cause fatigue during prolonged use. Since the phased array rotates along only a single axis, accommodating complex multi-axis hand movements is not currently supported. Also, excessive device movements during use may cause the device to rotate, preventing the phased array from properly orienting toward the hand.

In this section, we first present the typing interaction guidelines and the insights gained during the design and implementation of our proposed wearable UMH interface. Then, we propose interface guidelines for finger-specific UMH based on a detailed analysis of the experimental results. Lastly, we outline directions for future work to address the limitations mentioned earlier.

8.1 Design Guidelines for wearable Mid-air Haptic Interface-based VR Typing

8.1.1 Guidelines for Mid-air Haptic Interactions. Finger-level haptic feedback for VR typing As shown in Figure 13, there was no statistically significant difference in the key-press intervals and WPM between the ‘V’ condition and the ‘VH’ condition. However, as shown in Section 6.3.2, the results of the NASA-TLX showed statistically significant improvements in Performance and Frustration when combining visual feedback with haptic feedback. This finding aligns with the SUS questions and qualitative feedback results, as the SUS confidence-related question, “How well do you think you performed the task?” showed an improvement from 2.952 to 3.318 in the average score when combining visual with haptic feedback, an increase of approximately 12.40%. Additionally, post-interview feedback showed that 15 out of 24 participants responded positively, stating that “*Although it didn’t feel exactly like pressing a real keyboard, the feedback on each finger was helpful for typing.*”. These insights confirm that haptic feedback on each finger during typing contributed to a positive typing experience.

Typo-correction interaction for typing assistance Moreover, the time taken to correct typos showed a significant reduction, decreasing from an average of 1.536 seconds to 1.137 seconds (approximately a 25.98% decrease) with the proposed haptic feedback on the palm. Four participants also noted that tactile feedback was convenient in alerting them to typing errors. This suggests that the novel haptic feedback-based interaction using a wearable haptic interface can enhance the typing experience during VR typing. For instance, in the post-interview feedback, a participant mentioned that “*Without the tactile sensation, it was difficult to type because I had to visually check if my hand was in the correct key position.*”. To address this issue, novel interactions can be utilized, such as the hovering scenario introduced in the Use Case Scenario (Figure 14). Specifically, the system delivers a distinct tactile sensation when the hands are correctly positioned above the virtual keyboard, similar to the tactile markers on the ‘F’ and ‘J’ keys of a physical keyboard [26]. Another option is to provide feedback to the specific finger positioned over the next key to press, potentially improving the overall VR typing experience.

Need for additional input method As shown in Figure 13, haptic feedback did not affect the total error rate. To investigate the contributors of errors further, we conducted an in-depth analysis. The average Corrected Error Rate (CER) for each condition (V, H, and VH) was 10.77%, 9.835%, and 8.496%, respectively, with no statistically significant differences between conditions. Similarly, the Uncorrected Error Rate (UER) for each condition was 1.472%, 3.926%, and 0.356%, showing no statistical significance. Thus, these results indicate that haptic feedback does not influence typing errors. However, in the post-interview results, 8 participants identified unintended input as a primary contributor to distraction and interruption during typing, especially due to the keyboard mechanism that triggers input upon touch. These findings suggest that factors such as the accuracy and stability of hand visualization, as well as the input method and keyboard mechanism, impact error rates more significantly than haptic feedback alone in VR typing. This highlights the need for an augmented input method beyond simple collision detection-based keyboards, as a conventional virtual keyboard with haptic feedback is insufficient to reduce error rates. Therefore, we expect integrating gesture typing [17] or using a self-correction simulator [15] could enhance the user’s typing performance.

8.1.2 Guidelines for Finger-level Wearable Haptic Interface. Perceptible minimum intensity of UMH on the fingers Through measurement, simulation, and perception studies, we identified the minimum intensity required for effective finger-specific haptic interface design and developed a haptic interface that meets this threshold. In the user study (Figure 13), all participants except one reported that they could feel the UMH feedback during typing. This suggests that both the transducer size and the haptic rendering algorithm, which adjusts the phased array based on relative positioning, were valid and effective. Therefore, in future designs of wearable finger UMH interfaces, this perception threshold and interface design process can serve as a hardware guideline.

Issue related to weight Six participants cited weight as a drawback, which contributed to an increase in the NASA-TLX Physical Demand score, with average scores of 4.952 for ‘V’ and 5.727 for ‘VH’, indicating an increase of approximately 15.65%. Thus, reducing weight is a key challenge in designing a wearable UMH interface for

typing and requires additional research. The improvement methods and research directions are discussed in Section 8.2.

Challenges due to variations in user physiological differences and rotation Additionally, there exists another hardware challenge. We designed the interface to be adjustable and rotatable, allowing for customization based on individual physical characteristics such as hand size. However, despite these adjustments, the interface only rotates along a single axis and has a fixed length, which restricts its ability to accommodate the full range of wrist movements. Furthermore, inevitable axial rotation of the armband occurs due to user movement during use. This results in distortion of the feedback delivery space, even with the rotation of the interface. In the user study, we addressed this by instructing participants to wear the armband tightly and avoid excessive movement. However, for a robust wearable device, further research is needed to develop methods that ensure consistent feedback delivery despite the unavoidable rotation of the device during use. To address this, increasing the number of servo motors to enable 2-axis rotation [35] or incorporating linear movement into the interface would allow for more adaptive responses to the user's hand movements.

8.2 Future Work

As highlighted in the user study results, the primary factor reducing usability was the weight of the haptic interface. The phased array (120 g) constitutes 40% of the total weight, which can be reduced through hardware improvements. First, we can replace the current transducers (MA404S; 0.8 g) with smaller SMD type ones (MA40H1S; 0.1 g). Although this change would reduce tactile intensity by approximately 25%, reducing the transducer from a diameter of 10 mm and height of 7 mm to 5.2 mm × 5.2 mm × 1.15 mm yields a volume decrease of about 94.34%. Additionally, the haptic driver board for signal amplification can be miniaturized. By integrating voltage amplifiers directly with each transducer on the array, the need for a separate driver board would be eliminated [64, 75]. Additionally, both the transducer (28.5 g) and the interface (45.3 g) boards are manufactured with a thickness of 1.6 mm PCB. If we use a lightweight PCB with a thickness of 0.4 mm and replace all connectors and pins with direct wiring, the overall weight could be reduced by approximately 70 %. Furthermore, the weight can be reduced by lowering the internal density of the 3D-printed socket and using lightweight straps. As mentioned in Section 6.3.2, the comfort and weight of UltraBoard are within an acceptable range for use. However, these methods further minimize the weight, making it comparable to commercially available haptic gloves (138 g) [24].

Another limitation was the issue of accuracy in servo motor control within our proposed haptic rendering pipeline, which calls for research into approaches for refining the control of the servo motor. Currently, the phased array is positioned using a single servo motor, which rotates along one axis. By introducing additional servo motors, the system could support rotation across three axes, enabling precise alignment with the complex 3D movements of the arm and wrist [35]. This would allow the phased array to maintain effective position and orientation relative to the focal point, preserving feedback quality even as the phased array size is minimized. Since a larger phased array enables more compact and smaller focal point generation [12], further research is needed to identify an effective balance between the mechanical design that controls phased array positioning and the phased array size to manage the trade-off inherent in wearable UMH systems. This approach can also minimize usability differences due to individual anatomical variations.

Beyond these hardware improvements, we also see potential in bringing a variety of interactions with advanced haptic rendering techniques. For example, actuating multiple focal points could represent complex shapes and further enhance realism [6, 50]. Moreover, various levels of tactile intensity could be utilized to represent stiffness [38, 53].

9 CONCLUSION

To advance stationary UMH into a finger-level wearable UMH, it is essential to conduct UMH perception studies targeting the fingers and minimize the device's size. Therefore, we simulated the acoustic pressure generated by phased arrays of different shapes and sizes to identify the effective focal length and the phased array that supports wrist-worn and finger-specific feedback. Additionally, we conducted a finger-level perception study to determine the minimum feedback intensity perceivable on the fingertips and validated its feasibility. Finally, we present Ultraboard, a novel wearable haptic feedback system designed to provide finger-specific UMH feedback. Ultraboard is a haptic interface that consistently provides tactile feedback to the fingers, regardless of the user's hand movements or motions. To assess Ultraboard's subjective and objective performance, we conducted a user study involving a typing scenario. Our results showed a significant improvement in user confidence and preference, as the haptic feedback provided a clear cue for each keystroke. Notably, the newly introduced typo correction interaction significantly reduced typo correction time and was considered effective by several participants. These results suggest that our finger-targeted haptic feedback system shows the potential to deliver effective feedback in mid-air interactions. Our findings offer design and system guidelines for finger-level wearable UMH interface and VR typing interaction design. We hope this study lays a foundation for future research on wearable UMH systems, paving the way for a more compact and integrated wearable interface.

Acknowledgements

This work was partly supported by the Institute of Information & Communications Technology Planning & Evaluation (IITP)-ITRC (Information Technology Research Center) grant funded by the Korea government (MSIT) (IITP-2025-RS-2024-00436398, 50%) and Ministry of Culture, Sports and Tourism(MCST) and Korea Creative Content Agency (KOCCA) in the Culture Technology (CT) Research & Development Program 2023 (No.00216939, 50%).

REFERENCES

- [1] F Alnajjar, Qi An, Mohit Saravanan, Khaled Khalil, Munkhjargal Gochoo, and S Shimoda. 2022. The effect of visual, auditory, tactile and cognitive feedback in motor skill training: A pilot study based on VR gaming. In *Converging Clinical and Engineering Research on Neurorehabilitation IV: Proceedings of the 5th International Conference on Neurorehabilitation (ICNR2020), October 13–16, 2020*. Springer, 445–449. https://doi.org/10.1007/978-3-030-70316-5_71
- [2] Inc. Apple. 2024. Apple Vision Pro. <https://www.apple.com/apple-vision-pro/>
- [3] Hrvoje Benko, Christian Holz, Mike Sinclair, and Eyal Ofek. 2016. NormalTouch and TextureTouch: High-fidelity 3D Haptic Shape Rendering on Handheld Virtual Reality Controllers. In *Proceedings of the 29th Annual Symposium on User Interface Software and Technology (Tokyo, Japan) (UIST '16)*. Association for Computing Machinery, New York, NY, USA, 717–728. <https://doi.org/10.1145/2984511.2984526>
- [4] Zekai Liang Haoyang Zhang Qianchen Xia Liang Xie Huijiong Yan Fanqi Sun Huicheng Feng Kai Tao Qiang Shen Bowen Ji, Xuanqi Wang and Erwei Yin. 2024. Flexible Strain Sensor-Based Data Glove for Gesture Interaction in the Metaverse: A Review. *International Journal of Human-Computer Interaction* 40, 21 (2024), 6793–6812. <https://doi.org/10.1080/10447318.2023.2212232>
- [5] Daniel Brice, Thomas McRoberts, and Karen Rafferty. 2019. A proof of concept integrated multi-systems approach for large scale tactile feedback in VR. In *International Conference on Augmented Reality, Virtual Reality and Computer Graphics*. Springer, 120–137. https://doi.org/10.1007/978-3-030-25965-5_10
- [6] Tom Carter, Sue Ann Seah, Benjamin Long, Bruce Drinkwater, and Sriram Subramanian. 2013. UltraHaptics: multi-point mid-air haptic feedback for touch surfaces. In *Proceedings of the 26th Annual ACM Symposium on User Interface Software and Technology (St. Andrews, Scotland, United Kingdom) (UIST '13)*. Association for Computing Machinery, New York, NY, USA, 505–514. <https://doi.org/10.1145/2501988.2502018>
- [7] Daniel K.Y. Chen, Jean-Baptiste Chossat, and Peter B. Shull. 2019. HaptiVec: Presenting Haptic Feedback Vectors in Handheld Controllers using Embedded Tactile Pin Arrays. In *Proceedings of the 2019 CHI Conference on Human Factors in Computing Systems* (Glasgow, Scotland UK) (CHI '19). Association for Computing Machinery, New York, NY, USA, 1–11. <https://doi.org/10.1145/3290605.3300401>
- [8] Lung-Pan Cheng, Li Chang, Sebastian Marwecki, and Patrick Baudisch. 2018. iturk: Turning passive haptics into active haptics by making users reconfigure props in virtual reality. In *Proceedings of the 2018 CHI Conference on Human Factors in Computing Systems*. Association for Computing Machinery, New York, NY, USA, 1–10. <https://doi.org/10.1145/3173574.3173663>

- [9] Inrak Choi, Heather Culbertson, Mark R. Miller, Alex Olwal, and Sean Follmer. 2017. Grability: A Wearable Haptic Interface for Simulating Weight and Grasping in Virtual Reality. In *Proceedings of the 30th Annual ACM Symposium on User Interface Software and Technology* (Québec City, QC, Canada) (UIST '17). Association for Computing Machinery, New York, NY, USA, 119–130. <https://doi.org/10.1145/3126594.3126599>
- [10] Inrak Choi, Eyal Ofek, Hrvoje Benko, Mike Sinclair, and Christian Holz. 2018. CLAW: A Multifunctional Handheld Haptic Controller for Grasping, Touching, and Triggering in Virtual Reality. In *Proceedings of the 2018 CHI Conference on Human Factors in Computing Systems* (Montreal QC, Canada) (CHI '18). Association for Computing Machinery, New York, NY, USA, 1–13. <https://doi.org/10.1145/3173574.3174228>
- [11] Giulia Corniani and Hannes P. Saal. 2020. Tactile innervation densities across the whole body. *Journal of Neurophysiology* 124, 4 (2020), 1229–1240. <https://doi.org/10.1152/jn.00313.2020> PMID: 32965159.
- [12] Bruce W. Drinkwater. 2022. *The Physical Principles of Arrays for Mid-Air Haptic Applications*. Springer International Publishing, Cham, 313–334. https://doi.org/10.1007/978-3-031-04043-6_14
- [13] Bruce W. Drinkwater and Paul D. Wilcox. 2006. Ultrasonic arrays for non-destructive evaluation: A review. *NDT E International* 39, 7 (2006), 525–541. <https://doi.org/10.1016/j.ndteint.2006.03.006>
- [14] Tafadzwa Joseph Dube and Ahmed Sabbir Arif. 2023. Ultrasonic Keyboard: A Mid-Air Virtual Qwerty with Ultrasonic Feedback for Virtual Reality. In *Proceedings of the Seventeenth International Conference on Tangible, Embedded, and Embodied Interaction* (Warsaw, Poland) (TEI '23). Association for Computing Machinery, New York, NY, USA, Article 47, 8 pages. <https://doi.org/10.1145/3569009.3573117>
- [15] John Dudley, Hrvoje Benko, Daniel Wigdor, and Per Ola Kristensson. 2019. Performance Envelopes of Virtual Keyboard Text Input Strategies in Virtual Reality. In *2019 IEEE International Symposium on Mixed and Augmented Reality (ISMAR)*. 289–300. <https://doi.org/10.1109/ISMAR.2019.00027>
- [16] John J. Dudley, Keith Vertanen, and Per Ola Kristensson. 2018. Fast and Precise Touch-Based Text Entry for Head-Mounted Augmented Reality with Variable Occlusion. 25, 6, Article 30 (Dec. 2018), 40 pages. <https://doi.org/10.1145/3232163>
- [17] John J. Dudley, Jingyao Zheng, Aakar Gupta, Hrvoje Benko, Matt Longest, Robert Wang, and Per Ola Kristensson. 2023. Evaluating the Performance of Hand-Based Probabilistic Text Input Methods on a Mid-Air Virtual Qwerty Keyboard. *IEEE Transactions on Visualization and Computer Graphics* 29, 11 (oct 2023), 4567–4577. <https://doi.org/10.1109/TVCG.2023.3320238>
- [18] Cathy Fang, Yang Zhang, Matthew Dworman, and Chris Harrison. 2020. Wireality: Enabling complex tangible geometries in virtual reality with worn multi-string haptics. In *Proceedings of the 2020 CHI Conference on Human Factors in Computing Systems*. Association for Computing Machinery, New York, NY, USA, 1–10. <https://doi.org/10.1145/3313831.3376470>
- [19] William Frier, Damien Ablart, Jamie Chilles, Benjamin Long, Marcello Giordano, Marianna Obrist, and Sriram Subramanian. 2018. Using Spatiotemporal Modulation to Draw Tactile Patterns in Mid-Air. In *Haptics: Science, Technology, and Applications*, Domenico Prattichizzo, Hiroyuki Shinoda, Hong Z. Tan, Emanuele Ruffaldi, and Antonio Frisoli (Eds.). Springer International Publishing, Cham, 270–281. https://doi.org/10.1007/978-3-319-93445-7_24
- [20] William Frier, Dario Pittera, Damien Ablart, Marianna Obrist, and Sriram Subramanian. 2019. Sampling Strategy for Ultrasonic Mid-Air Haptics. In *Proceedings of the 2019 CHI Conference on Human Factors in Computing Systems* (Glasgow, Scotland Uk) (CHI '19). Association for Computing Machinery, New York, NY, USA, 1–11. <https://doi.org/10.1145/3290605.3300351>
- [21] Ravichandran Gayathri and Sanghun Nam. 2024. Enhancing User Experience in Virtual Museums: Impact of Finger Vibrotactile Feedback. *Applied Sciences* 14, 15 (2024). <https://doi.org/10.3390/app14156593>
- [22] Janet K. Gibbs, Marco Gillies, and Xueni Pan. 2022. A comparison of the effects of haptic and visual feedback on presence in virtual reality. *International Journal of Human-Computer Studies* 157 (2022), 102717. <https://doi.org/10.1016/j.ijhcs.2021.102717>
- [23] Hyunjae Gil, Hyungki Son, Jin Ryong Kim, and Ian Oakley. 2018. Whiskers: Exploring the Use of Ultrasonic Haptic Cues on the Face. In *Proceedings of the 2018 CHI Conference on Human Factors in Computing Systems* (Montreal QC, Canada) (CHI '18). Association for Computing Machinery, New York, NY, USA, 1–13. <https://doi.org/10.1145/3173574.3174232>
- [24] MANUS Technology Group. 2023. Manus Prime3 Haptic XR. <https://www.manus-meta.com/products/prime-3-haptic-xr>
- [25] Aakar Gupta, Majed Samad, Kenrick Kin, Per Ola Kristensson, and Hrvoje Benko. 2020. Investigating Remote Tactile Feedback for Mid-Air Text-Entry in Virtual Reality. In *2020 IEEE International Symposium on Mixed and Augmented Reality (ISMAR)*. 350–360. <https://doi.org/10.1109/ISMAR50242.2020.00062>
- [26] Aakar Gupta, Naveen Sendhilnathan, Jess Hartcher-O'Brien, Evan Pezent, Hrvoje Benko, and Tanya R Jonker. 2023. Investigating eyes-away mid-air typing in virtual reality using squeeze haptics-based postural reinforcement. In *Proceedings of the 2023 CHI Conference on Human Factors in Computing Systems*. Association for Computing Machinery, New York, NY, USA, 1–11. <https://doi.org/10.1145/3544548.3581467>
- [27] Sidhant Gupta, Dan Morris, Shwetak N. Patel, and Desney Tan. 2013. AirWave: non-contact haptic feedback using air vortex rings. In *Proceedings of the 2013 ACM International Joint Conference on Pervasive and Ubiquitous Computing* (Zurich, Switzerland) (UbiComp '13). Association for Computing Machinery, New York, NY, USA, 419–428. <https://doi.org/10.1145/2493432.2493463>
- [28] Sandra G. Hart and Lowell E. Staveland. 1988. Development of NASA-TLX (Task Load Index): Results of Empirical and Theoretical Research. 52 (1988), 139–183. [https://doi.org/10.1016/S0166-4115\(08\)62386-9](https://doi.org/10.1016/S0166-4115(08)62386-9)

- [29] Keisuke Hasegawa and Hiroyuki Shinoda. 2013. Aerial display of vibrotactile sensation with high spatial-temporal resolution using large-aperture airborne ultrasound phased array. In *2013 World Haptics Conference (WHC)*. IEEE, 31–36. <https://doi.org/10.1109/WHC.2013.6548380>
- [30] Keisuke Hasegawa and Hiroyuki Shinoda. 2018. Aerial Vibrotactile Display Based on Multiunit Ultrasound Phased Array. *IEEE Transactions on Haptics* 11, 3 (2018), 367–377. <https://doi.org/10.1109/TOH.2018.2799220>
- [31] Seongkook Heo, Christina Chung, Geehyuk Lee, and Daniel Wigdor. 2018. Thor’s Hammer: An Ungrounded Force Feedback Device Utilizing Propeller-Induced Propulsive Force. In *Proceedings of the 2018 CHI Conference on Human Factors in Computing Systems* (Montreal QC, Canada) (*CHI ’18*). Association for Computing Machinery, New York, NY, USA, 1–11. <https://doi.org/10.1145/3173574.3174099>
- [32] Juan David Hincapié-Ramos, Xiang Guo, Paymahn Moghadasian, and Pourang Irani. 2014. Consumed endurance: a metric to quantify arm fatigue of mid-air interactions (*CHI ’14*). Association for Computing Machinery, New York, NY, USA, 1063–1072. <https://doi.org/10.1145/2556288.2557130>
- [33] Takayuki Hoshi. 2022. Introduction to ultrasonic mid-air haptic effects. In *Ultrasound Mid-Air Haptics for Touchless Interfaces*. Springer, 1–20. https://doi.org/10.1007/978-3-031-04043-6_1
- [34] Takayuki Hoshi, Takayuki Iwamoto, and Hiroyuki Shinoda. 2009. Non-contact tactile sensation synthesized by ultrasound transducers. In *World Haptics 2009 - Third Joint EuroHaptics conference and Symposium on Haptic Interfaces for Virtual Environment and Teleoperator Systems*. 256–260. <https://doi.org/10.1109/WHC.2009.4810900>
- [35] Thomas Howard, Maud Marchal, Anatole Lécuyer, and Claudio Pacchierotti. 2019. PUMAH: pan-tilt ultrasound mid-air haptics for larger interaction workspace in virtual reality. *IEEE transactions on haptics* 13, 1 (2019), 38–44. <https://doi.org/10.1109/TOH.2019.2963028>
- [36] Thomas Howard, Maud Marchal, and Claudio Pacchierotti. 2022. Ultrasound mid-air tactile feedback for immersive virtual reality interaction. In *Ultrasound Mid-Air Haptics for Touchless Interfaces*. Springer, 147–183. https://doi.org/10.1007/978-3-031-04043-6_6
- [37] Hsin-Yu Huang, Chih-Wei Ning, Po-Yao Wang, Jen-Hao Cheng, and Lung-Pan Cheng. 2020. Haptic-go-round: A surrounding platform for encounter-type haptics in virtual reality experiences. In *Proceedings of the 2020 CHI Conference on Human Factors in Computing Systems*. Association for Computing Machinery, New York, NY, USA, 1–10. <https://doi.org/10.1145/3313831.3376476>
- [38] Inwook Hwang, Hyunki Son, and Jin Ryong Kim. 2017. AirPiano: Enhancing music playing experience in virtual reality with mid-air haptic feedback. In *2017 IEEE World Haptics Conference (WHC)*. 213–218. <https://doi.org/10.1109/WHC.2017.7989903>
- [39] Hyunyoung Jang, Jinwook Kim, and Jeongmi Lee. 2024. Effects of Congruent Multisensory Feedback on the Perception and Performance of Virtual Reality Hand-Retargeted Interaction. *IEEE Access* 12 (2024), 119789–119802. <https://doi.org/10.1109/ACCESS.2024.3450512>
- [40] Sujin Jang, Wolfgang Stuerzlinger, Satyajit Ambike, and Karthik Ramani. 2017. Modeling Cumulative Arm Fatigue in Mid-Air Interaction based on Perceived Exertion and Kinetics of Arm Motion. In *Proceedings of the 2017 CHI Conference on Human Factors in Computing Systems* (Denver, Colorado, USA) (*CHI ’17*). Association for Computing Machinery, New York, NY, USA, 3328–3339. <https://doi.org/10.1145/3025453.3025523>
- [41] Roland S. Johansson and Åke B. Vallbo. 1979. Tactile sensibility in the human hand: relative and absolute densities of four types of mechanoreceptive units in glabrous skin. *The Journal of Physiology* 286 (1979). <https://api.semanticscholar.org/CorpusID:9264175>
- [42] Farzan Kalantari, David Gueorguiev, Edward Lank, Nicolas Bremard, and Laurent Grisoni. 2018. Exploring Fingers’ Limitation of Texture Density Perception on Ultrasonic Haptic Displays. In *Haptics: Science, Technology, and Applications*, Domenico Prattichizzo, Hiroyuki Shinoda, Hong Z. Tan, Emanuele Ruffaldi, and Antonio Frisoli (Eds.). Springer International Publishing, Cham, 354–365. https://doi.org/10.1007/978-3-319-93445-7_31
- [43] Brian Kappus and Ben Long. 2018. Spatiotemporal modulation for mid-air haptic feedback from an ultrasonic phased array. *The Journal of the Acoustical Society of America* 143, 3_Supplement (2018), 1836–1836. <https://doi.org/10.1121/1.5036027>
- [44] Yaesol Kim, Hyun Jung Kim, and Young J Kim. 2018. Encountered-type haptic display for large VR environment using per-plane reachability maps. *Computer Animation and Virtual Worlds* 29, 3-4 (2018), e1814. <https://doi.org/10.1002/cav.1814>
- [45] Georgios Korres and Mohamad Eid. 2016. Haptogram: Ultrasonic point-cloud tactile stimulation. *IEEE Access* 4 (2016), 7758–7769. <https://doi.org/10.1109/ACCESS.2016.2608835>
- [46] Ruiheng Lan, Xu Sun, Qingfeng Wang, and Bingjian Liu. 2024. Ultrasonic Mid-Air Haptics on the Face: Effects of Lateral Modulation Frequency and Amplitude on Users’ Responses. In *Proceedings of the CHI Conference on Human Factors in Computing Systems* (Honolulu, HI, USA) (*CHI ’24*). Association for Computing Machinery, New York, NY, USA, Article 712, 12 pages. <https://doi.org/10.1145/3613904.3642417>
- [47] Jaeyeon Lee, Mike Sinclair, Mar Gonzalez-Franco, Eyal Ofek, and Christian Holz. 2019. TORC: A virtual reality controller for in-hand high-dexterity finger interaction. In *Proceedings of the 2019 CHI conference on human factors in computing systems*. Association for Computing Machinery, New York, NY, USA, 1–13. <https://doi.org/10.1145/3290605.3300301>
- [48] H. Levitt. 1971. Transformed Up-Down Methods in Psychoacoustics. *The Journal of the Acoustical Society of America* 49, 2B (02 1971), 467–477. <https://doi.org/10.1121/1.1912375>
- [49] Chungman Lim, Gunhyuk Park, and Hasti Seifi. 2024. Designing Distinguishable Mid-Air Ultrasound Tactons with Temporal Parameters. In *Proceedings of the CHI Conference on Human Factors in Computing Systems*. Association for Computing Machinery, New York, NY, USA, 1–18. <https://doi.org/10.1145/3613904.3642522>

- [50] Benjamin Long, Sue Ann Seah, Tom Carter, and Sriram Subramanian. 2014. Rendering volumetric haptic shapes in mid-air using ultrasound. *ACM Trans. Graph.* 33, 6, Article 181 (nov 2014), 10 pages. <https://doi.org/10.1145/2661229.2661257>
- [51] Tiffany Luong, Yi Fei Cheng, Max Möbus, Andreas Fender, and Christian Holz. 2023. Controllers or Bare Hands? A Controlled Evaluation of Input Techniques on Interaction Performance and Exertion in Virtual Reality. *IEEE Transactions on Visualization and Computer Graphics* (2023). <https://doi.org/doi=10.1109/TVCG.2023.3320211>
- [52] I Scott MacKenzie and R William Soukoreff. 2003. Phrase sets for evaluating text entry techniques. In *CHI'03 extended abstracts on Human factors in computing systems*. Association for Computing Machinery, New York, NY, USA, 754–755. <https://doi.org/10.1145/765891.765971>
- [53] M. Marchal, G. Gallagher, A. Lécuyer, and C. Pacchierotti. 2020. Can Stiffness Sensations Be Rendered in Virtual Reality Using Mid-air Ultrasound Haptic Technologies?. In *Haptics: Science, Technology, Applications*, Ilana Nisky, Jess Hartcher-O'Brien, Michaël Wiertlewski, and Jeroen Smeets (Eds.). Springer International Publishing, Cham, 297–306. https://doi.org/10.1007/978-3-030-58147-3_33
- [54] Asier Marzo, Tom Corkett, and Bruce W. Drinkwater. 2018. Ultraino: An Open Phased-Array System for Narrowband Airborne Ultrasound Transmission. *IEEE Transactions on Ultrasonics, Ferroelectrics, and Frequency Control* 65, 1 (2018), 102–111. <https://doi.org/10.1109/TUFFC.2017.2769399>
- [55] Inc. Meta Platforms. [n. d.]. Meta Horizon Unity Documentation. <https://developers.meta.com/horizon/documentation/unity/VK-unity-overview/> Accessed: 2024-10-31.
- [56] Inc. Meta Platforms. 2023. Meta Quest3. <https://www.meta.com/quest/quest-3/>
- [57] Inc. Meta Platforms. 2024. Meta Quest3s. <https://www.meta.com/quest/quest-3s/>
- [58] Saya Mizutani, Masahiro Fujiwara, Yasutoshi Makino, and Hiroyuki Shinoda. 2019. Thresholds of Haptic and Auditory Perception in Midair Facial Stimulation. In *2019 IEEE International Symposium on Haptic, Audio and Visual Environments and Games (HAVE)*. 1–6. <https://doi.org/10.1109/HAVE.2019.8920999>
- [59] Lendy Mulot, Thomas Howard, Guillaume Gicquel, Claudio Pacchierotti, and Maud Marchal. 2024. Bimanual Ultrasound Mid-Air Haptics for Virtual Reality Manipulation. *IEEE Transactions on Visualization and Computer Graphics* (2024). <https://doi.org/10.1109/TVCG.2024.3417343>
- [60] Marianna Obrist, Sriram Subramanian, Elia Gatti, Benjamin Long, and Thomas Carter. 2015. Emotions mediated through mid-air haptics. In *Proceedings of the 33rd annual ACM conference on human factors in computing systems*. Association for Computing Machinery, New York, NY, USA, 2053–2062. <https://doi.org/10.1145/2702123.2702361>
- [61] OptiTrack, NaturalPoint Inc. n.d. OptiTrack Motion Capture Systems. <https://www.optitrack.com/>.
- [62] Konstantina Orfanou, Nikolaos Tselios, and Christos Katsanos. 2015. Perceived usability evaluation of learning management systems: Empirical evaluation of the System Usability Scale. *The International Review of Research in Open and Distributed Learning* 16, 2 (2015). <https://doi.org/10.19173/irrodl.v16i2.1955>
- [63] Claudio Pacchierotti, Stephen Sinclair, Massimiliano Solazzi, Antonio Frisoli, Vincent Hayward, and Domenico Prattichizzo. 2017. Wearable Haptic Systems for the Fingertip and the Hand: Taxonomy, Review, and Perspectives. *IEEE Transactions on Haptics* 10, 4 (2017), 580–600. <https://doi.org/10.1109/TOH.2017.2689006>
- [64] Karri Palovuori, Ismo Rakkolainen, and Antti Sand. 2014. Bidirectional touch interaction for immaterial displays. In *Proceedings of the 18th International Academic MindTrek Conference: Media Business, Management, Content & Services (Tampere, Finland) (AcademicMindTrek '14)*. Association for Computing Machinery, New York, NY, USA, 74–76. <https://doi.org/10.1145/2676467.2676503>
- [65] Kevin Pan, William Frier, and Deepak Sahoo. 2022. *Ultrasound Mid-Air Haptic Feedback at the Fingertip*. Springer International Publishing, Cham, 299–311. https://doi.org/10.1007/978-3-031-04043-6_13
- [66] David Panzoli, Paco Royeres, and Mathéo Fedou. 2019. Hand-based interactions in Virtual Reality: No better feeling than the real thing!. In *2019 11th International Conference on Virtual Worlds and Games for Serious Applications (VS-Games)*. 1–2. <https://doi.org/10.1109/VS-Games.2019.8864546>
- [67] J. Perret and E. Vander Poorten. 2018. Touching virtual reality: a review of haptic gloves. In *ACTUATOR 2018; 16th International Conference on New Actuators*. VDE, 1–5.
- [68] Evan Pezent, Ali Israr, Majed Samad, Shea Robinson, Priyanshu Agarwal, Hrvoje Benko, and Nick Colonnese. 2019. Tasbi: Multisensory Squeeze and Vibrotactile Wrist Haptics for Augmented and Virtual Reality. In *2019 IEEE World Haptics Conference (WHC)*. 1–6. <https://doi.org/10.1109/WHC.2019.8816098>
- [69] Ismo Rakkolainen, Ahmed Farooq, Jari Kangas, Jaakko Hakulinen, Jussi Rantala, Markku Turunen, and Roope Raisamo. 2021. Technologies for multimodal interaction in extended reality—a scoping review. *Multimodal Technologies and Interaction* 5, 12 (2021), 81. <https://doi.org/10.3390/mti5120081>
- [70] Ismo Rakkolainen, Euan Freeman, Antti Sand, Roope Raisamo, and Stephen Brewster. 2021. A Survey of Mid-Air Ultrasound Haptics and Its Applications. *IEEE Transactions on Haptics* 14, 1 (2021), 2–19. <https://doi.org/10.1109/TOH.2020.3018754>
- [71] Sonja Rümelin, Thomas Gabler, and Jesper Bellenbaum. 2017. Clicks are in the Air: How to Support the Interaction with Floating Objects through Ultrasonic Feedback. In *Proceedings of the 9th International Conference on Automotive User Interfaces and Interactive Vehicular Applications (Oldenburg, Germany) (AutomotiveUI '17)*. Association for Computing Machinery, New York, NY, USA, 103–108. <https://doi.org/10.1145/3122986.3123010>

- [72] Jonghyun Ryu. 2010. Psychophysical model for vibrotactile rendering in mobile devices. *Presence: Teleoper. Virtual Environ.* 19, 4 (Aug. 2010), 364–387. https://doi.org/10.1162/PRES_a_00011
- [73] Steeven Villa Salazar, Claudio Pacchierotti, Xavier de Tinguy, Anderson Maciel, and Maud Marchal. 2020. Altering the stiffness, friction, and shape perception of tangible objects in virtual reality using wearable haptics. *IEEE transactions on haptics* 13, 1 (2020), 167–174. <https://doi.org/10.1109/TOH.2020.2967389>
- [74] Majed Samad and Ladan Shams. 2016. Visual–somatotopic interactions in spatial perception. *Neuroreport* 27, 3 (2016), 180–185. <https://doi.org/10.1097/WNR.0000000000000521>
- [75] Antti Sand, Ismo Rakkolainen, Poika Isokoski, Jari Kangas, Roope Raisamo, and Karri Palovuori. 2015. Head-mounted display with mid-air tactile feedback. In *Proceedings of the 21st ACM symposium on virtual reality software and technology*. Association for Computing Machinery, New York, NY, USA, 51–58. <https://doi.org/10.1145/2821592.2821593>
- [76] Aaron Raymond See, Jose Antonio G Choco, and Kohila Chandramohan. 2022. Touch, texture and haptic feedback: a review on how we feel the world around us. *Applied Sciences* 12, 9 (2022), 4686. <https://doi.org/10.3390/app12094686>
- [77] Qijia Shao, Amy Sniffen, Julien Blanchet, Megan E. Hillis, Xinyu Shi, Themistoklis K. Haris, Jason Liu, Jason Lamberton, Melissa Malzkuhn, Lorna C. Quandt, James Mahoney, David J. M. Kraemer, Xia Zhou, and Devin Balkcom. 2020. Teaching American Sign Language in Mixed Reality. *Proc. ACM Interact. Mob. Wearable Ubiquitous Technol.* 4, 4, Article 152 (Dec. 2020), 27 pages. <https://doi.org/10.1145/3432211>
- [78] Vivian Shen, Craig Shultz, and Chris Harrison. 2022. Mouth Haptics in VR using a Headset Ultrasound Phased Array. In *Proceedings of the 2022 CHI Conference on Human Factors in Computing Systems* (New Orleans, LA, USA) (CHI '22). Association for Computing Machinery, New York, NY, USA, Article 275, 14 pages. <https://doi.org/10.1145/3491102.3501960>
- [79] Zhouyang Shen, Zak Morgan, Madhan Kumar Vasudevan, Marianna Obrist, and Diego Martinez Plasencia. 2024. Controlled-STM: A Two-stage Model to Predict User’s Perceived Intensity for Multi-point Spatiotemporal Modulation in Ultrasonic Mid-air Haptics. In *Proceedings of the CHI Conference on Human Factors in Computing Systems* (Honolulu, HI, USA) (CHI '24). Association for Computing Machinery, New York, NY, USA, Article 709, 12 pages. <https://doi.org/10.1145/3613904.3642439>
- [80] Bukun Son and Jaeyoung Park. 2018. Haptic Feedback to the Palm and Fingers for Improved Tactile Perception of Large Objects. In *Proceedings of the 31st Annual ACM Symposium on User Interface Software and Technology* (Berlin, Germany) (UIST '18). Association for Computing Machinery, New York, NY, USA, 757–763. <https://doi.org/10.1145/3242587.3242656>
- [81] Patrick L Strandholt, Oana A Dogaru, Niels C Nilsson, Rolf Nordahl, and Stefania Serafin. 2020. Knock on wood: Combining redirected touching and physical props for tool-based interaction in virtual reality. In *Proceedings of the 2020 CHI Conference on Human Factors in Computing Systems*. Association for Computing Machinery, New York, NY, USA, 1–13. <https://doi.org/10.1145/3313831.3376303>
- [82] Chongyang SUN, Weizhi NAI, and Xiaoying SUN. 2019. Tactile sensitivity in ultrasonic haptics: Do different parts of hand and different rendering methods have an impact on perceptual threshold? *Virtual Reality Intelligent Hardware* 1, 3 (2019), 265–275. <https://doi.org/10.3724/SP.J.2096-5796.2019.0009> Human-computer interactions for virtual reality.
- [83] Youjin Sung, Rachel Kim, Kun Woo Song, Yitian Shao, and Sang Ho Yoon. 2024. HapticPilot: Authoring In-situ Hand Posture-Adaptive Vibrotactile Feedback for Virtual Reality. *Proc. ACM Interact. Mob. Wearable Ubiquitous Technol.* 7, 4, Article 179 (Jan. 2024), 28 pages. <https://doi.org/10.1145/3631453>
- [84] Shun Suzuki, Masahiro Fujiwara, Yasutoshi Makino, and Hiroyuki Shinoda. 2019. Midair ultrasound haptic display with large workspace. In *Haptic Interaction: Perception, Devices and Algorithms* 3. Springer, 3–5. https://doi.org/10.1007/978-981-13-3194-7_1
- [85] Ryoko Takahashi, Keisuke Hasegawa, and Hiroyuki Shinoda. 2018. Lateral Modulation of Midair Ultrasound Focus for Intensified Vibrotactile Stimuli. In *Haptics: Science, Technology, and Applications*, Domenico Prattichizzo, Hiroyuki Shinoda, Hong Z. Tan, Emanuele Ruffaldi, and Antonio Frisoli (Eds.). Springer International Publishing, Cham, 276–288. https://doi.org/10.1007/978-3-319-93399-3_25
- [86] Yi Tang, Jialu Xu, Qiutong Liu, Xiaodan Hu, Wenhao Xue, Zhirui Liu, Ziyi Lin, Hancong Lin, Yili Zhang, Zhuang Zhang, Xuezhi Ma, Jing Wang, Junwen Zhong, Dangxiao Wang, Hanqing Jiang, and Yuan Ma. 2024. Advancing haptic interfaces for immersive experiences in the metaverse. *Device* 2, 6 (2024), 100365. <https://doi.org/10.1016/j.device.2024.100365>
- [87] Alvin R Tilley. 2001. *The measure of man and woman: human factors in design*. John Wiley & Sons.
- [88] Ultraleap. 2019. Stratos Explore: A New Way to Create and Deliver Mid-Air Haptics. <https://www.ultraleap.com/company/news/press-release/stratos-explore/>
- [89] Nicha Vanichvoranun, Hojeong Lee, Seoyeon Kim, and Sang Ho Yoon. 2024. EStatiG: Wearable Haptic Feedback with Multi-Phalanx Electrostatic Brake for Enhanced Object Perception in VR. *Proc. ACM Interact. Mob. Wearable Ubiquitous Technol.* 8, 3, Article 131 (Sept. 2024), 29 pages. <https://doi.org/10.1145/3678567>
- [90] Steeven Villa, Sven Mayer, Jess Hartcher-O’Brien, Albrecht Schmidt, and Tonja-Katrin Machulla. 2022. Extended Mid-air Ultrasound Haptics for Virtual Reality. *Proc. ACM Hum.-Comput. Interact.* 6, ISS, Article 578 (Nov. 2022), 25 pages. <https://doi.org/10.1145/3567731>
- [91] Haokun Wang, Yatharth Singhal, Hyunjae Gil, and Jin Ryong Kim. 2024. Fiery Hands: Designing Thermal Glove through Thermal and Tactile Integration for Virtual Object Manipulation. In *Proceedings of the 37th Annual ACM Symposium on User Interface Software and Technology* (Pittsburgh, PA, USA) (UIST '24). Association for Computing Machinery, New York, NY, USA, Article 101, 15 pages. <https://doi.org/10.1145/3654777.3676457>

- [92] Xizi Wang, Ben Lafreniere, and Jian Zhao. 2024. Exploring Visualizations for Precisely Guiding Bare Hand Gestures in Virtual Reality. In *Proceedings of the 2024 CHI Conference on Human Factors in Computing Systems* (Honolulu, HI, USA) (CHI '24). Association for Computing Machinery, New York, NY, USA, Article 636, 19 pages. <https://doi.org/10.1145/3613904.3642935>
- [93] Chyanna Wee, Kian Meng Yap, and Woan Ning Lim. 2021. Haptic interfaces for virtual reality: Challenges and research directions. *IEEE access* 9 (2021), 112145–112162. <https://doi.org/10.1109/ACCESS.2021.3103598>
- [94] Graham Wilson, Thomas Carter, Sriram Subramanian, and Stephen A. Brewster. 2014. Perception of ultrasonic haptic feedback on the hand: localisation and apparent motion. In *Proceedings of the SIGCHI Conference on Human Factors in Computing Systems* (Toronto, Ontario, Canada) (CHI '14). Association for Computing Machinery, New York, NY, USA, 1133–1142. <https://doi.org/10.1145/2556288.2557033>
- [95] Gareth Young, Hamish Milne, Daniel Griffiths, Elliot Padfield, Robert Blenkinsopp, and Orestis Georgiou. 2020. Designing Mid-Air Haptic Gesture Controlled User Interfaces for Cars. *Proc. ACM Hum.-Comput. Interact.* 4, EICS, Article 81 (June 2020), 23 pages. <https://doi.org/10.1145/3397869>
- [96] Mengjia Zhu, Amirhossein H. Memar, Aakar Gupta, Majed Samad, Priyanshu Agarwal, Yon Visell, Sean J. Keller, and Nicholas Colonnese. 2020. PneuSleeve: In-fabric Multimodal Actuation and Sensing in a Soft, Compact, and Expressive Haptic Sleeve. In *Proceedings of the 2020 CHI Conference on Human Factors in Computing Systems* (Honolulu, HI, USA) (CHI '20). Association for Computing Machinery, New York, NY, USA, 1–12. <https://doi.org/10.1145/3313831.3376333>

Appendix A SERVO MOTOR CONTROL ALGORITHM

Algorithm 1 illustrates the servo motor control within the haptic rendering pipeline, which consists of servo motor control and UMH generation.

Algorithm 1 Servo motor control algorithm

Input

▶ OptriTrack Tracking Data

- $fingertipSet_left = \{P_{thumb_left}, P_{index_left}, P_{middle_left}, P_{ring_left}, P_{pinky_left}\}$
- $fingertipSet_right = \{P_{thumb_right}, P_{index_right}, P_{middle_right}, P_{ring_right}, P_{pinky_right}\}$
- $arraySet_left = \{P_{left\ phased\ array}: 4\ vertexes\ of\ phased\ array\}$.
- $arraySet_right = \{P_{right\ phased\ array}: 4\ vertexes\ of\ phased\ array\}$.

Output

- Adjusted position of each $arraySet$.

for each $fingertipSet$, $arraySet$ in **Input do**

Initialize $\vec{N}_{phased\ array}$ from $P_{arraySet}$

for each fingertip f from P_{thumb} through P_{pinky} **do**

Let L be an imaginary line parallel to the upper edge of the phased array and passing through the center

$$\vec{V}_f = \min(\vec{L}f)$$

$$\theta_f = \cos^{-1} \left(\frac{\vec{N}_{phased\ array} \cdot \vec{V}_f}{|\vec{N}_{phased\ array}| |\vec{V}_f|} \right)$$

end for

if the fingertip P_f with the largest θ is not within the phased array's space volume **then**

if P_f is above the phased array **then**

Move the phased array farther from the current hand.

else if P_f is below the phased array **then**

Move the phased array closer to the current hand.

end if

else

for each fingertip f in $fingertipSet$ **do**

Find the fingertip f_{min} with minimum distance $d_{min} = \|f_{min} - P_{phased\ array, hand}\|$

if $d_{min} < 12$ **then**

Move the phased array farther from the fingertip f_{min} on the current hand.

else if $d_{min} > 18$ **then**

Move the phased array closer to the fingertip f_{min} on the current hand.

end if

end for

end if

end for

return Adjusted $phased\ array$ for both left and right hands.

Appendix B SIMULATION FOR FOCAL LENGTH

Figure 15 shows the simulation and intensity of acoustic pressure generated at different focal lengths.

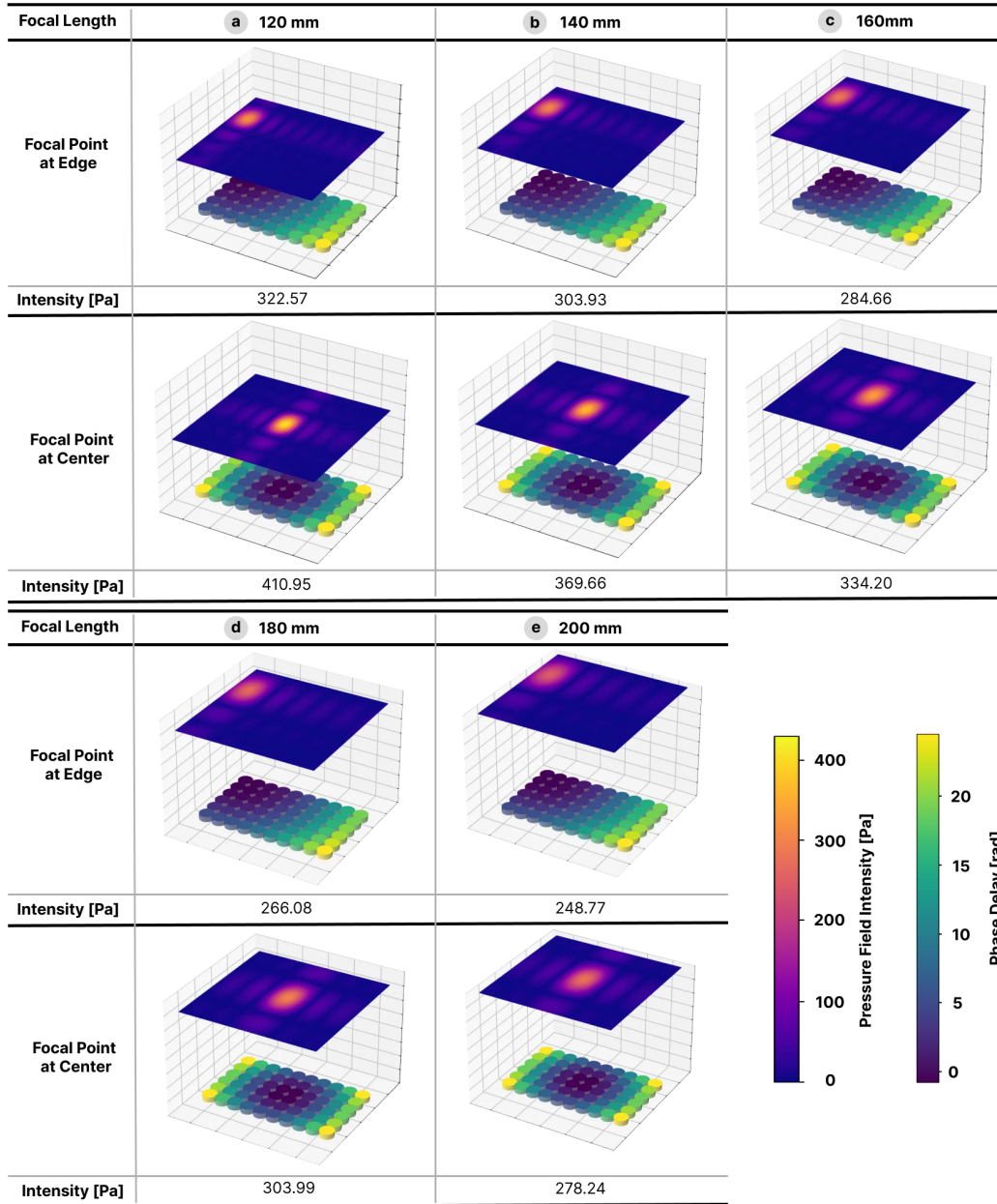


Fig. 15. Simulations conducted at various focal lengths. (a) 120 mm, (b) 140 mm, (c) 160 mm, (d) 180 mm, (e) 200 mm